Successive, large mass-transport deposits in the south Kermadec fore-arc basin, New Zealand: The Matakaoa Submarine Instability Complex

Geoffroy Lamarche

National Institute of Water and Atmospheric Research (NIWA) Ltd, Private Bag 14–901, Wellington 6241, New Zealand (g.lamarche@niwa.co.nz)

Cathy Joanne and Jean-Yves Collot

Géosciences Azur, Université de Nice Sophia–Antipolis, Institut de Recherche pour le Développement (IRD), Université Pierre et Marie Curie, Centre National de la Recherche Scientifique (CNRS), Observatoire de la Côte d'Azur, B.P. 48, F–06235 Villefranche-sur–Mer Cédex, France

[1] Four >100 km³ mass-transport deposits (MTDs) identified from their morphology and seismic facies across the Matakaoa Margin and Raukumara fore-arc basin, NE New Zealand, constitute the Matakaoa Submarine Instability Complex (MSIC). MSIC originates from a 45-km-wide, 1100-m-high reentrant in the continental slope. The deposits resulted from three mass-failure events: (1) The Raukumara Slump is identified from the collapsed NW flank of an anticline at the northern end of the reentrant and imbricate structures at its distal end, overlying a flat décollement over a >50-km distance. The slump age is roughly estimated between upper Miocene and lower Pleistocene. (2) The Matakaoa Debris Avalanche (MDA) is subdivided into a ~260-km³ blocky unit and a ~170-km³ weakly reflective unit, overlying a high-amplitude seismic reflector truncating the underlying sedimentary units. The MDA is dated 600 ± 150 ka. It originated as a slump, as indicated by back-tilted blocks overlying a rotational failure surface, and evolved during transport as a debris avalanche. The failure of sedimentary basement blocks released Plio-Pleistocene shelf-basin infill, thus producing the blocky and weakly reflective units. Fore-arc basin sediments deformed in front of the MDA for approximately 20 km. (3) The Matakaoa Debris Flow (MDF) occurred 38–100 ka ago and extends 200 km northward from the reentrant headwall and consists of a 150-m-thick layer with a chaotic seismic facies. Scouring beneath the MDF and a <250-m-high east bounding scarp indicate basal and lateral erosion associated with the flow displacement. Incorporation of eroded material into the debris flow accounts for >30% of the flow's 1250 km³ volume. Factors facilitating failures include the following: slope oversteepening associated with margin uplift and fore-arc subsidence, large-scale folding related to shortening between the Pacific and Australia plates, high-discharge rivers draining the region, and rapid sediment accumulation on the margin. Large to great earthquakes along the plate interface are a likely trigger mechanism controlling the recurrence of large margin failures. Unlike other MTDs along plate boundaries, which are destined to be consumed into the subduction factory, the MSIC provides an opportunity to investigate mega-instabilities at an active margin over million year timescales.

1. Introduction

[2] "Mass-transport deposit" (MTD) is a generic term referring to geological material that is rapidly remobilized from and redeposited on the seafloor and typically implies slope failure and gravitational deformation in the form of downslope mass movements and flows. "Submarine landslides" and "seafloor failures" are generic terms used in the literature to refer to processes that lead to MTDs [*Canals et al.*, 2004; *Coleman and Prior*, 1988; *Hampton et al.*, 1996; *Mulder and Cochonat*, 1996; *Nardin et al.*, 1979], and these terms are used interchangeably in this study. Processes leading to MTDs can be simplified in three classes [*Hampton et al.*, 1996; *McHugh et al.*, 2002; *Nardin et al.*, 1979; *Schwartz*, 1982; *Mulder and Cochonat*, 1996]: (1) rockfalls, including debris avalanches, characterized by individual blocks [e.g., *Masson et al.*, 2002]; (2) slides and slumps, where shear failure occurs along a discrete sliding surface with little internal deformation; and (3) mass flows, including mud and debris flows, where internal deformation resulting from laminar fluid-like motion is extensive [*Dasgupta*, 2003; *Prior et al.*, 1984]. Turbidites also originate from submarine instabilities and are controlled by gravitational movement to form sediment deposits. Turbidites, however, are not mass transport deposits as they are generated by fluid flows where motion is supported by turbulence. Different types of MTDs can occur in the same environment to form mass transport complexes, and examples of avalanche/slump complexes [*Masson et al.*, 2002], debris avalanches and debris flows [e.g., *Collot et al.*, 2001], slumps and debris flows [*Jenner et al.*, 2007; *Piper et al.*, 1999; *Piper and McCall*, 2003] and multiple deposits [*Moscardelli et al.*, 2006] are numerous. Several transport and depositional processes may occur simultaneously or sequentially [*Nardin et al.*, 1979]. Therefore, mass movements evolve during transport from their initial failure, and consequently, similar deposits can originate from different failure and transport mechanisms, e.g., debris flows evolving into turbidity currents [*Felix and Peakall*, 2006; *Mohrig and Marr*, 2003], slides evolving into debris flows [*Masson et al.*, 1998; *Prior et al.*, 1984], and slumps evolving into debris avalanches (this study).

[3] The seismic characters of MTDs provide substantial information regarding their mode of failure and transport. Indeed, there is a continuum in the seismic character of MTDs [*Nardin et al.*, 1979]. The spatial dimensions of MTDs in the marine environment spans several orders of magnitude in area (up to 10^{10} m²), and volume (10^3–10^{12} m³), which suits the use of seismic reflection imaging techniques for their identification. Runout distances of MTDs may be several hundred kilometers. Submarine MTDs therefore, represent major dynamic responses of the seafloor to tectonic (e.g., earthquakes, uplift/subsidence), and sedimentary or climatic forcings. Their study can provide critical constraints for establishing global sediment budgets along continental margins, understanding the mechanisms of sediment redistribution and landscape evolution as well as improving our knowledge of geological hazards.

[4] Large submarine MTDs have been observed in many different environments, including along volcanoes flanks [*Moore et al.*, 1989, 1994] and submarine fans [*Maslin et al.*, 1998; *Piper et al.*, 1997], but most commonly occur along continental slopes [*Canals et al.*, 2004]. A number of factors are required to generate mass transport in the marine environment and these commonly combine on continental slopes of active convergent margins [e.g., *Collot et al.*, 2001; *McAdoo et al.*, 2000]. Here, tectonic erosion, high fluid pressures and the occurrence of gas hydrates, large earthquakes and high sedimentation rates all contribute to slope instability. On timescales greater than approximately 500 ka, however, the study of large landslides at convergent margins is hindered by the subduction process, whereby the remobilized masses are destined to disappear either through subduction or accretion processes, and examples of MTDs are not often preserved in the sedimentary record [*Collot et al.*, 2001].

[5] The Matakaoa Submarine Instability Complex (MSIC), however, has developed along the northeast active margin of New Zealand and has been

preserved because it is deposited outside the inner trench wall (Figure 1). Consequently, the MSIC offers an excellent opportunity to investigate large submarine landslides in the geodynamical context of an active convergent margin.

[6] In this paper, we describe the upper Neogene and Quaternary history of the MSIC from the interpretation of a comprehensive set of multibeam bathymetric data and multichannel seismic (MCS) reflection profiles acquired between 2001 and 2003. These data provide pseudo three-dimensional information on the topography and geological structures of the submarine area north of the Raukumara Peninsula, described herein as the Matakaoa Margin (Figure 1). We identify the geometry and extent of different components of the MSIC, their geological and stratigraphic relationships and reconstruct the margin morphology prior to failures. In particular, we describe the morphology and structure of the Matakaoa Reentrant and the adjacent Raukumara Basin to unravel the complex system of instabilities and the factors controlling the evolution of MTDs in general. The succession of three large failures and the development of an age model further enable us to discuss the recurrence of large MTDs at million year timescales.

2. Geological Setting of the Matakaoa Margin

[7] We propose the name ''Matakaoa Margin'' as the region encompassing the narrow (6- to 15-km-wide), E−W trending, continental shelf and the continental slope between the Raukumara Peninsula and the flat seafloor of the Raukumara Basin

to the south and north, respectively (Figure 1). The margin is located at the complex intersection of three geological and geodynamic domains: the southern Kermadec-Hikurangi Margin, the Raukumara Basin and the Raukumara Peninsula.

[8] The southern Kermadec-northern Hikurangi margin, east of the Raukumara Peninsula, marks the active convergent Pacific-Australia plate boundary (Figure 1). The continental slope consists of a nongrowing oversteepened accretionary wedge, dissected by margin-parallel strike-slip faults [*Collot and Davy*, 1998]. Tectonic erosion and active faulting are driven essentially by the subduction of the ~13- to 15-km-thick oceanic crust of the Hikurangi Plateau, which is heavily studded with volcanic edifices [*Davy*, 1992; *Wood and Davy*, 1994].

[9] North of East Cape, the 2500-m-deep Raukumara Basin represents the fore-arc basin of the southern Kermadec subduction system. The basin has at least 8 km of sediment infill [*Davey et al.*, 1997; *Gillies and Davey*, 1986]. To the west, the Raukumara Basin is bounded by the active volcanic arc of the Kermadec Ridge [*Wright*, 1994]. To the east, the basin is separated from the slope of the southern Kermadec margin by a NNE trending system of continental basement highs, formed by Ranfurly Bank and the East Cape Ridge (Figure 1).

[10] The subduction of the Hikurangi Plateau with protruding seamounts is associated with underplating of material beneath the Raukumara Peninsula which has resulted in a widespread uplift of the upper plate, and exposure of fore-arc material in the Raukumara Peninsula (Figure 1) [*Mazengarb and Speden*, 2000; *Reyners and McGinty*, 1999].

Figure 1. The East Cape region, NE New Zealand. The area is located approximately 80 km to the west of the Hikurangi Trough (HIK), which represents the Pacific-Australia (PAC/AUS) convergent plate boundary (thick grey line with teeth indicating upper plate). The Raukumara Basin (RB) is the expression of the fore-arc basin associated with subduction of the Pacific Plate (PAC) along the Southern Kermadec Trench (SKT), whereas the onland Raukumara Peninsula is uplifting in association with the subduction of the 15-km-thick volcanic Hikurangi Plateau (inset) along the Hikurangi Trough. The Raukumara Peninsula extends to the NE along the continental Ranfurly Bank (RBk) and East Cape Ridge (ECR). The extents of the Ruatoria Debris Avalanche (thick black and white contour) and debris flow (dotted patterns) are from *Collot et al.* [2001] and *Lewis et al.* [2004]. The extent of the Matakaoa Debris Flow is from *Carter* [2001] and this study. The Matakaoa Reentrant (MR) is indenting the Matakaoa Margin located north of the Raukumara Peninsula. The Waipaoa (Wa), Uwa (Uw), and Waiapu (Wu) rivers together discharge 70.10^6 t of sediment per year on the continental shelf [*Hicks and Shankar*, 2003; *Orpin et al.*, 2006] and particularly into the Waiapu faulted shelf basin (WB) [*Addington et al.*, 2007; *Lewis et al.*, 2004]. Frame indicates location of Figure 2. Inset: the Pacific-Australia Plate boundary along the Hikurangi and Southern Kermadec margins. The triangular region located between the Kermadec-Hikurangi margin and the Havre Trough (HT) forms the Kermadec micro plate (KER). The relative plate motion between KER and PAC at a rate of 54 mm/a is indicated by the N277°E vector [*Collot et al.*, 2001; *De Mets et al.*, 1994]. The northern and southern boundaries of the Hikurangi Plateau are indicated by thick grey dashed lines. The Taupo Volcanic Zone (TVZ) is the location of volcanic ashes (tephra) recognized in cores and used for dating the MDA (see text).

Elevated marine terraces and river cuttings indicate gradual uplift along the east coast of the peninsula to its axis, with a maximum rate of 2.6 mm/a at the northern coast (Figure 1) [*Gibb*, 1981; *Wilson et al.*, 2007a, 2007b] and 3.3. mm/a along the Raukumara Axial Ranges [*Lewis et al.*, 2004]. Geophysical modeling suggests that the subducted Hikurangi Plateau lies approximately 20 km beneath East Cape [*Reyners and McGinty*, 1999].

[11] The Matakaoa Margin is subject to high seismic activity. However, because of the weak interplate coupling in the region *Reyners* [1998] and *Reyners and McGinty* [1999] estimate the maxi-
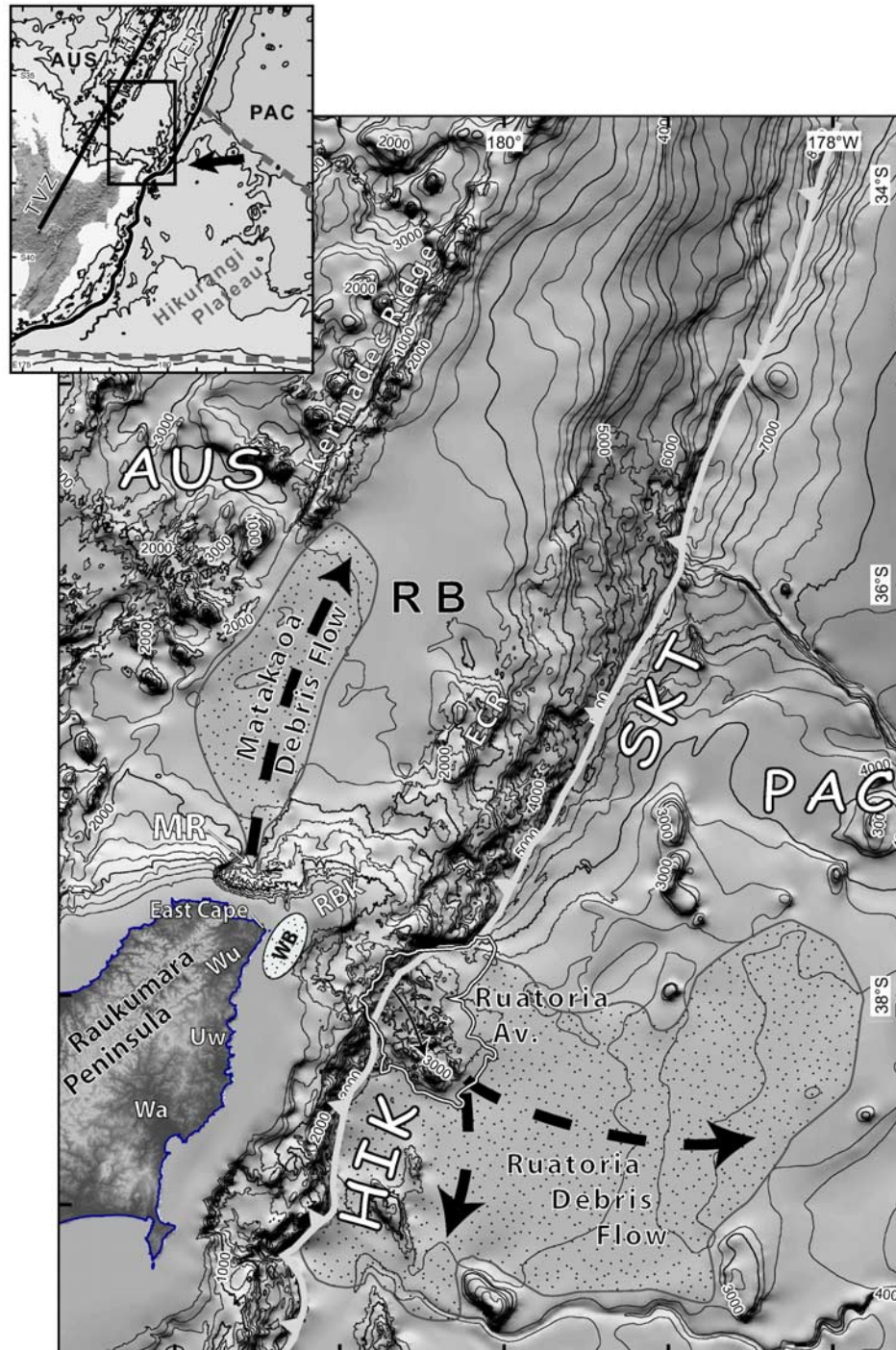

Figure 1

mum possible magnitude of a subduction thrust event in the region is M_W 6.9. Paleoseismicity studies in the Hawkes Bay region, ~100 km to the south, indicate likely M_W 7.9 earthquakes on the subduction interface at ~7100 and 5550 years B.P. [*Cochran et al.*, 2006], whereas elastic-dislocation models suggest that rupture of the entire 500 km plate boundary along the North Island would produce a M_W 8.3 earthquake (U. A. Cochran, personal communication, 2007).

[12] The basic stratigraphy and structure of the upper margin consists of a succession of well-bedded, highly reflective sequences, separated by basal unconformities which correspond to indurated Mesozoic greywackes and autochthonous Paleogene strata, together with early Miocene slide sheets of the East Coast Allochthon [*Field et al.*, 1997]. These units were tectonically faulted and folded during the Quaternary, so that shelf and slope basins are filled with Neogene and Quaternary sediment. Fault-controlled shelf and slope basins are observed elsewhere along the North Island east coast continental shelf [*Lewis et al.*, 2004; *Orpin*, 2004]. Seismic reflection profiles indicate that very high sedimentation rates persisted through most of the Quaternary, with ~1 km of sediment fill accumulating in the Waiapu shelf basin immediately east of East Cape (Figure 1) [*Lewis et al.*, 2004].

[13] Late Quaternary sedimentation rates of 0.1–0.2 mm/a were estimated offshore in the Raukumara Basin [*Carter*, 2001; *Kohn and Glasby*, 1978]. On the continental shelf, sedimentation rates in the order of 0.5 mm/a are estimated from post–last glacial sediment thickness in the Waiapu shelf basin [*Lewis et al.*, 2004]. This basin is located at the head of the Ruatoria and the Matakaoa reentrants, to the east and north. Collapse and transverse structures in the Waiapu shelf basin (location on Figure 1) [*Lewis et al.*, 2004] are interpreted as evidence for the passage of a large subducting seamount beneath the continental shelf landward

of the head of the Ruatoria reentrant and support the hypothesis that the Ruatoria debris avalanche was formed in the wake of an obliquely subducting seamount [*Collot et al.*, 2001]. Holocene sedimentation rates reflect the high terrestrial input from the rapidly rising onshore Raukumara Ranges delivered to the continental shelf by the Waiapu River, New Zealand's largest fluvial supply of suspended load with 36 10^6 t of sediment discharged per year [*Hicks and Shankar*, 2003].

3. Data Sets

[14] We utilized a combination of multibeam bathymetry and MCS reflection data acquired during three oceanographic surveys (August 2001, April 2002, April 2003) on board R/V *Tangaroa*, over the Matakaoa Margin and the Raukumara Basin (Figure 2). The multibeam bathymetry was acquired using a SIMRAD EM300 and covers approximately 14000 km^2. Approximately 1100 km of MCS reflection data were acquired with 16 profiles acquired in 2001 (Mat101 to Mat116), and 10 profiles acquired in 2003 (Mat301 to Mat310) (Figure 2). The MCS equipment comprised one GI air gun operating in harmonic mode (45–105 in^3 chambers), and a 48-channel, 600-m-long analogue seismic streamer. Seismic processing included time domain filtering, predictive deconvolution, 12-fold stack, and time migration using velocity obtained from stacking velocity (NMO) analysis. The 10–250 Hz frequency range of the seismic system provides information to approximately 1.5 km beneath the seafloor with a resolution of less than ~5 m at depth shallower than 500 ms (note: all seismic reflection times are expressed in two-way travel-time). We also use archived seismic reflection data, essentially single-channel air-gun profiles, and several deep MCS oil industry profiles. A series of short gravity cores (<6 m) and dredge samples were acquired at specific targets with the aim of constraining the age of the various remobilized masses. High-resolution

Figure 2. Multibeam seafloor topography of the Matakaoa Margin and Raukumara Basin, with locations of seismic reflection profiles, core (star), and dredge (arrow) sites. The Digital Terrain Model (DTM) constructed from EM300 multibeam data is superimposed on contour lines from the regional bathymetry with contour lines providing a depth scale. White bold numbers indicate multichannel seismic profiles shown in subsequent figures (prefix Mat for seismic lines omitted for clarity). OGS Explora [*Davey et al.*, 1997] multichannel and Geodynz [*Collot et al.*, 1996] single-channel seismic reflection profiles were acquired for academic purposes and included in this interpretation, along with Mobil (Mob) and NZ Ministry of Economic Development (MED) deep industrial multichannel seismic reflection profiles. A number of other minor seismic reflection profiles were utilized [see *Carter*, 2001]. High-resolution 3.5 kHz profiles are not shown although they were systematically acquired along multibeam ship tracks. Inset: single-channel air gun profile over the toe of the Matakaoa Debris Flow (with location on main DTM) [from *Carter*, 2001].
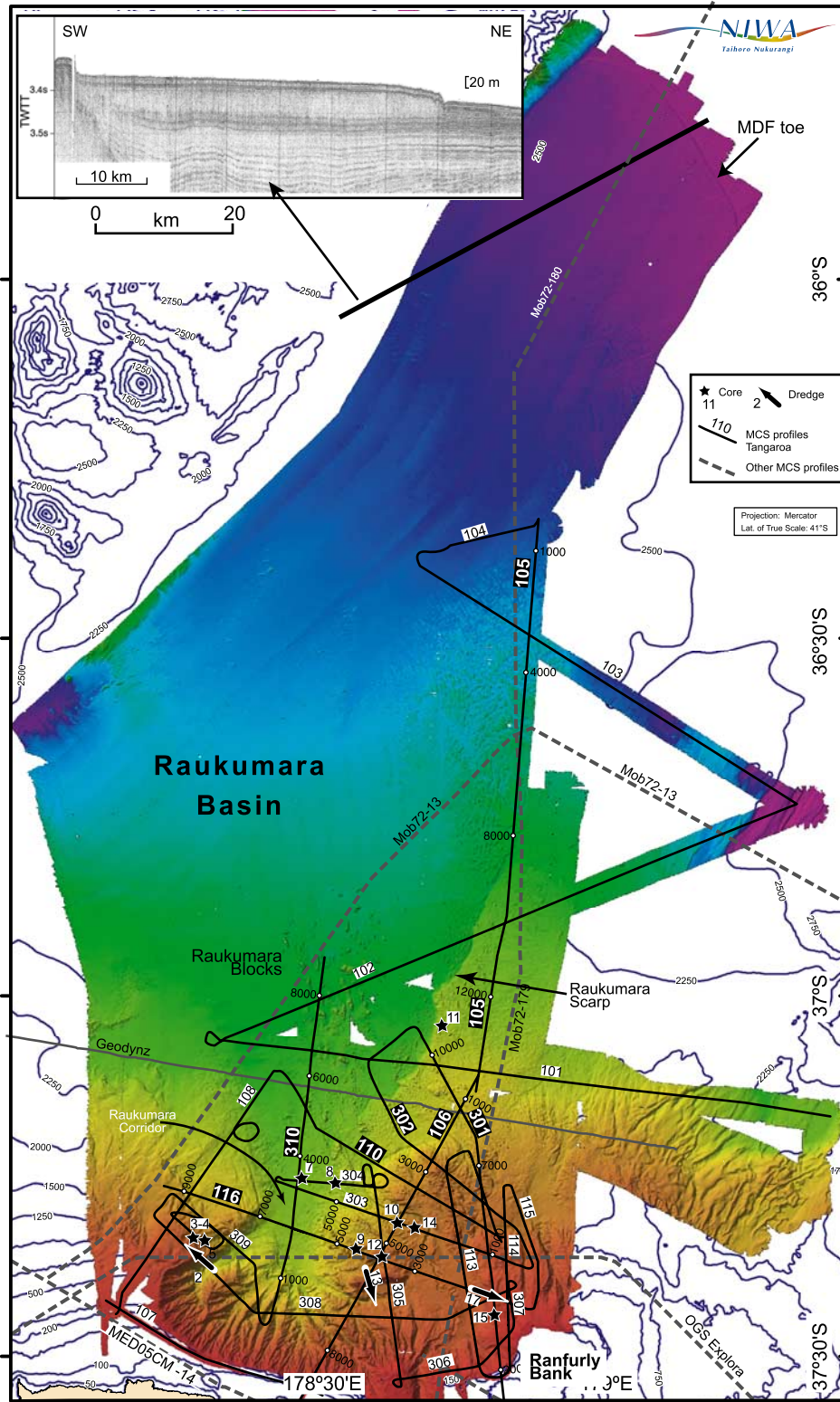
Figure 2

(3.5 kHz) seismic reflection data were acquired simultaneously with MCS and multibeam data.

4. Geomorphic Elements of the Continental Slope

[15] The Matakaoa Reentrant was first recognized from regional bathymetry and limited single-channel seismic reflection profiles [*Carter*, 2001; *Lewis and Marshall*, 1996]. The reentrant is a conspicuous 45-km-long, ~30-km-wide elliptic indentation of the Matakaoa Margin, which covers an area of ~1000 km^2 (Table 2), and divides into morphologically distinct eastern and western halves (Figure 3). The reentrant is delimited to the west by an 1100-m-high, NE trending, rectilinear wall and to the east by a 300-m-high, N trending scarp, concave to the west. Along its southern wall, the top of the head scarp lies in less than 250 m of water depth, less than 10 km from the coast of the Raukumara Peninsula. The reentrant is partly closed to the north and northeast by a zone of rugged terrain that rises up to ~1200 m water depth, and is called the Tokata Dome. To the west, the reentrant opens into the Raukumara Basin through a 2000-m-deep, 10-km-wide zone of flat-lying seafloor, herein named the Raukumara Corridor. The irregular continental slope east of the Matakaoa Reentrant descends from ~100 m at the top of Ranfurly Bank into the ~2300-m-deep Raukumara Basin.

[16] The reentrant's eastern half is characterized by a 1200-m-deep, ~300 km^2 area of smooth seafloor, cut by the meandering Matakaoa Channel. The channel terminates in the south at the linear, ~300-m-deep, 1-km-wide Matakaoa Canyon that incises the top of the continental slope (Figure 3). The southern wall of the eastern half of the reentrant is dissected by fan-valleys diverging downslope. The centre of the reentrant is dominated by several kilometer-wide hummocks, knolls and ridges. The largest ridge is the Matakaoa Ridge, a prominent 2-km-wide, ~10-km-long east trending ridge. Smaller ridges to the north, typically 2–3 km long, have a general E–W trend. The western half of the reentrant is characterized by the Raukumara Corridor to the north, and a steep southern wall, dissected by a pervasive network of slope canyons that radially converge downslope into the corridor. The average slope of the southern head wall is 7° (Figure 4).

[17] West of the Matakaoa Reentrant the upper continental slope has not been affected by large slope failures and can therefore be considered as a reference for prefailure slope morphology (Figure 3 and profile 1 on Figure 4a). The slope here has a concave-downward profile, with an average slope of 4°, whereas the lower slope has a gradient of less than 1° and merges progressively with the seafloor of the Raukumara Basin (Figure 4a, profile 1).

[18] North of the reentrant, the Raukumara Basin shows a very smooth and flat, approximately 2300-m-deep, seafloor extending at least 200 km to the north and north-west. A well-defined, 250-m-high, NNE trending scarp, herein called the Raukumara Scarp, straddles the seafloor of the Raukumara Basin, from immediately north of the reentrant for about 70 km (Figure 2). At the base of the scarp (west), the seafloor is scattered with blocks and ridges up to 800-m-long (e.g., 37°05′S/178°39′E, Figure 3) that trend parallel to the scarp. Further to the west, the seafloor is largely featureless, except for a cluster of about 60 large hummocks (up to 2.5 km long and 200 m high, e.g., 36°58′S/178°33′E, Figures 2 and 3) which arrange in map view to form a 40-km-long, pear-shaped field pointing southward named herein the Raukumara Blocks (Figure 2).

5. Continental Slope and Raukumara Basin Sedimentary Sequence and Structure

5.1. Basal Sedimentary Sequence

[19] A series of anticlines, with E–W axes (Figure 3) and controlled by steep reverse faults are visible beneath the continental slope of Ranfurly Bank (CDPs 3000, 5000 and 7000, Figure 5), the northernmost of which is called Tokata Anticline (CDP 2800 Figure 6). The Tokata Dome is the morphological expression of the outcropping summit of the anticline. Several seismically transparent lenses along the northern flanks of these anticlines are interpreted as small-scale MTDs (length <10 km; thickness <100 m).

[20] The sedimentary sequence beneath the continental slope and the Raukumara Basin is imaged on MCS profiles to approximately 2 s (2–2.5 km) beneath the seafloor. We recognize upper and lower sedimentary units and an acoustic basement (Table 1, Figures 5 to 10). Both sedimentary units have comparable seismic character, consisting of highly coherent, high-amplitude reflectors. The base of the upper sedimentary unit is an unconformity identified as a series of onlaps in the core of
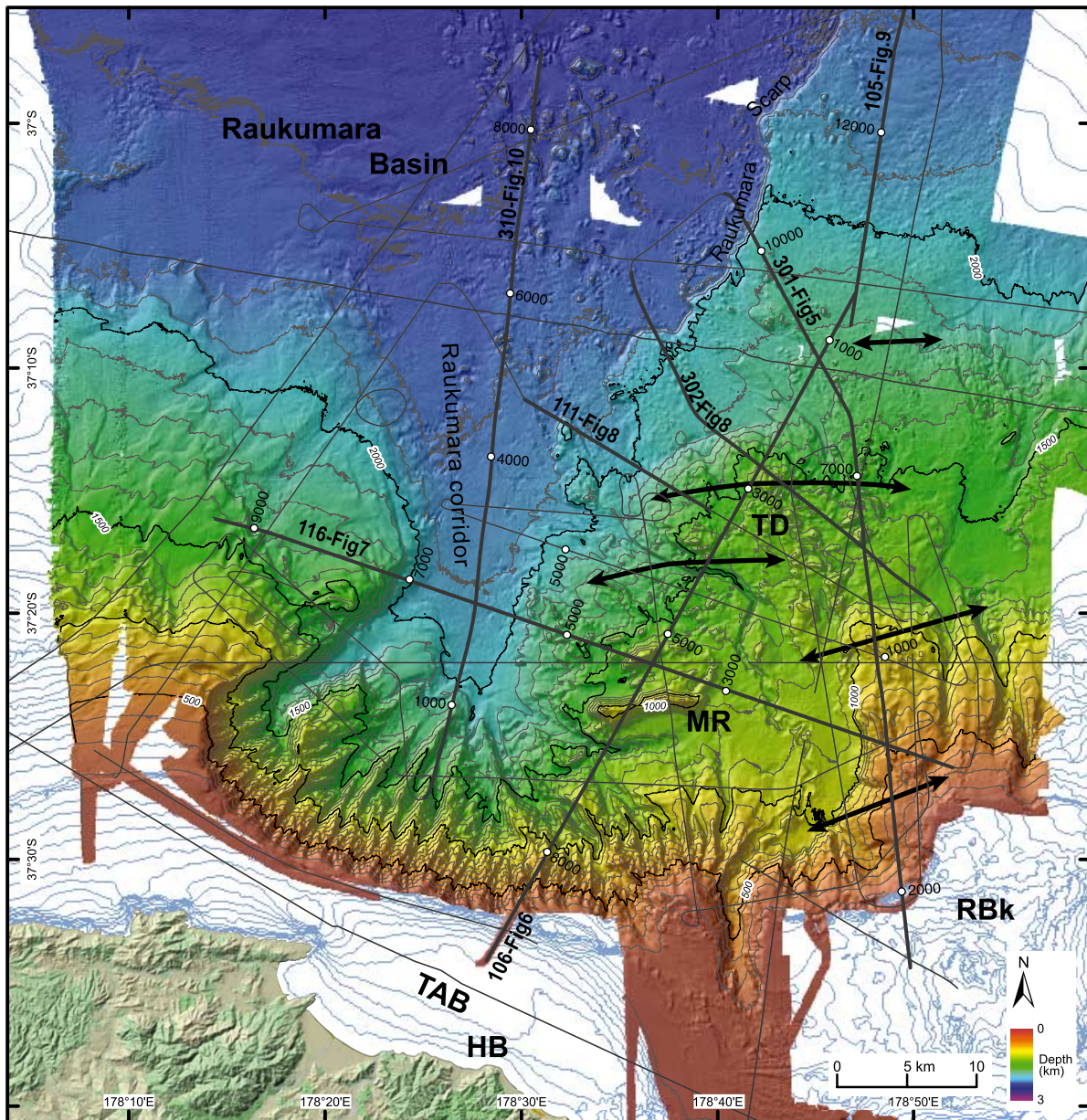
Figure 3. EM300 multibeam bathymetry over the region of the Matakaoa Reentrant. The 25-m grid is shaded from the north and superimposed on the contoured regional bathymetry. Multichannel seismic reflection profiles are indicated by thick lines with CDP numbers, line numbers (prefix Mat omitted), and figure numbers only for profiles shown in subsequent figures, and in thin, light grey for those not shown in this paper. Double arrows indicate anticline axes as interpreted from seismic reflection profiles. Main topographic features discussed in text include Matakaoa Ridge (MR), Ranfurly Bank (RBk), and Te Aroha shelf Basin (TAB). The Tokata Dome (TD) is the morphologic expression of the Tokata Anticline. Horoera Bay (HB) is the location of inferred 2.6 mm/a Holocene uplift [*Wilson et al.*, 2007a]. Onshore data are derived from Eagle Technology Ltd.'s EagleData[TM], which is a derivative of the 1:50,000 Digital Vector Topographic Land Information New Zealand data set.

the Tokata Anticline (CDP2800, Figure 6) indicating that tectonic deformation initiated prior to the deposition of the upper sedimentary unit. Folding within the upper sedimentary unit indicates syn-deformation sedimentation. In the reentrant, the upper and lower sedimentary units have ~500 ms and ~1100 ms minimum thicknesses, respectively,

and the tops of both units are truncated (Figure 6). Both units extend northward into the Raukumara Basin where the top of the upper unit is truncated.

[21] Both sedimentary units rise beneath the reentrant eastern wall (Figures 7 and 8a). The prominent folds of the sedimentary sequence observed
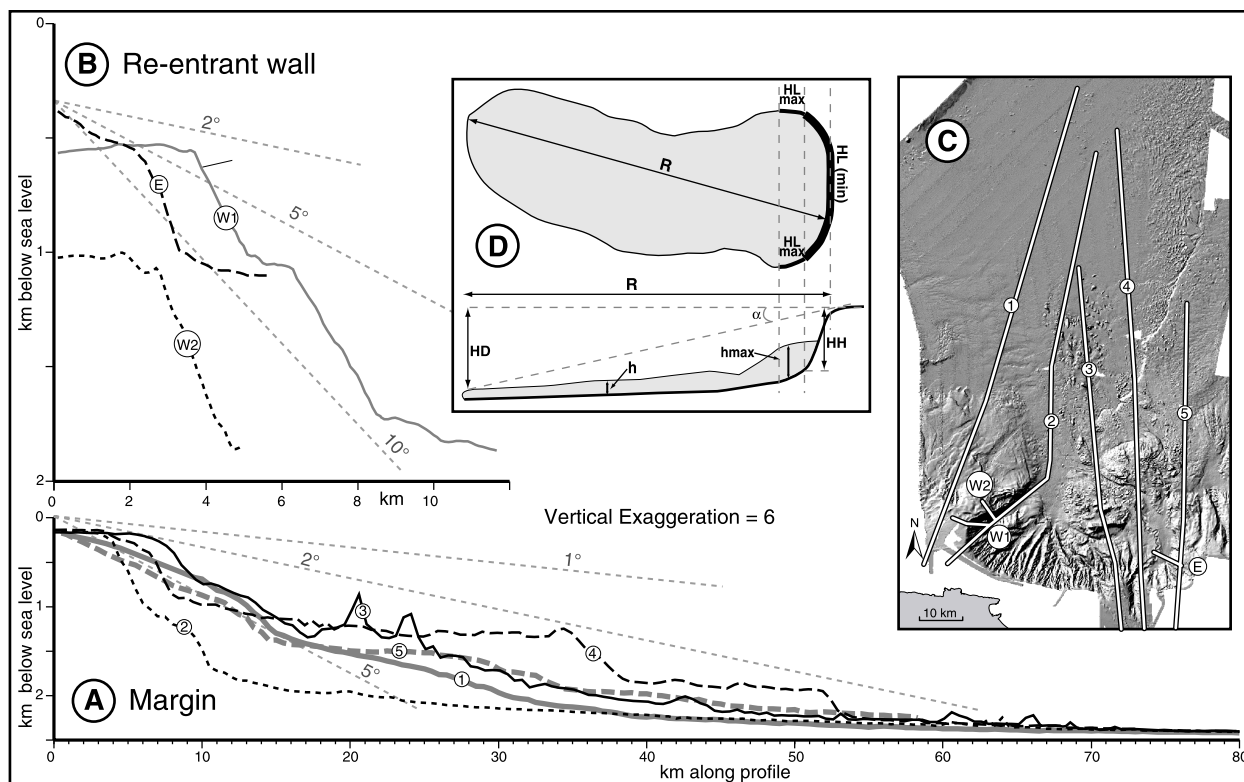
Figure 4. Bathymetric profiles across the margin and the reentrant. (a) The Matakaoa Margin includes the continental slope on either side of the reentrant (profiles 1 and 5, i.e., along the nonfailed parts of the margin) and within the reentrant (profiles 2, 3, and 4). (b) Western and eastern reentrant walls. (c) Map showing profile locations. (d) Sketch of the various morphometric parameters used in text and Tables 2 and 3.

beneath the reentrant and Ranfurly Bank attest to a compressional tectonic environment. Beneath the reentrant's headwall, both upper and lower sedimentary units are sharply truncated subvertically over ~700 ms beneath the southern rim of the reentrant (CDP 7800, Figure 6), ~500 ms to the east (CDP 1500 Figure 7), and 200 ms to the west (CDP 1600, Figure 10).

5.2. Quaternary Sequences

[22] The top of the continental slope is characterized by subhorizontal reflectors that prograde northward (Postavalanche Sediment Wedge (PSW), Figure 5c) and unconformably overlie a slope basin. The eastern scarp of the reentrant has a slope of 18° and truncates the Ranfurly Bank sedimentary sequence (profile E, Figure 4b).

[23] The eastern part of the reentrant is underlain by a <300-ms-thick seismic unit characterized by interfingering, high-amplitude, low-frequency, coherent reflectors, interpreted as turbidite deposits with typical levees on both sides of the Matakaoa

Channel (Figures 3 and 7). A wedge of sediment is ensconced within the southern wall of the reentrant, and tapers northward with an average surface slope of 4.5° (PSW on Figures 6 and 7). In cross section, the sediment wedge consists of a package of high-frequency, conformable reflectors unconformably overlying the underlying units.

6. Morphology and Structures of the Matakaoa Submarine Instability Complex

[24] From the seafloor morphology (Figures 2 and 3), and seismic facies, we identify five distinct large MTDs (i.e., >100 km^3, Table 1) along the Matakaoa Margin and in the Raukumara Basin, which together make the Matakaoa Submarine Instability Complex (MSIC). From their geometrical relationships, we demonstrate that the five MTDs originate from three distinct major submarine mass-failure events: (1) the Raukumara Slump; (2) the Matakaoa Debris Avalanche (MDA); and (3) the Matakaoa Debris Flow (MDF).
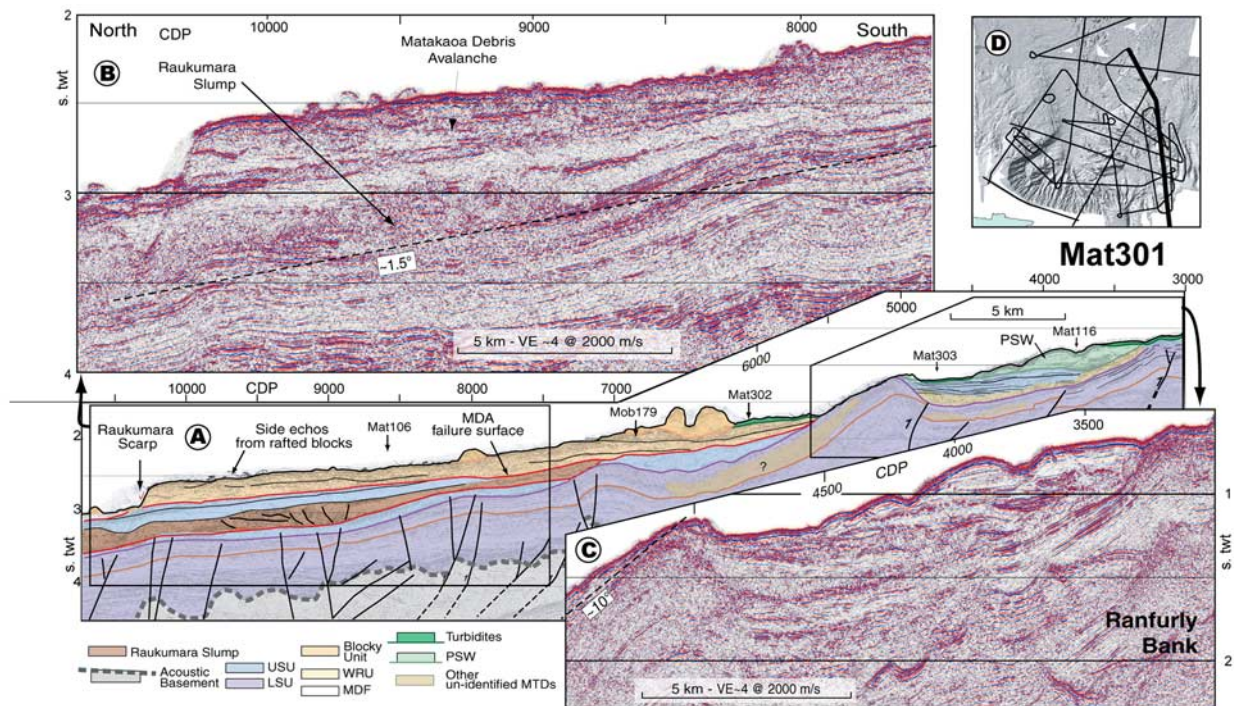
Figure 5. MCS reflection profile Mat301 along the eastern edge of the Matakaoa Reentrant and southern part of the Raukumara Basin. (a) Interpreted profile. (b) Enlargement of uninterpreted fully processed seismic data over the distal part of the Matakaoa Debris Avalanche (MDA). (c) Enlargement of uninterpreted fully processed seismic data over the upper part of the margin. See (d) inset and Figure 2 for location of seismic profiles. All seismic data were processed using Globe Claritas™ from GNS Science, Lower Hutt, NZ. Slope gradients are calculated using sound velocities of 1800 m/s in the Matakaoa Debris Avalanche and 2000 m/s in underlying units. MDF, Matakaoa Debris Flow; WRU, Weakly Reflective Unit; LSU, Lower Sedimentary Unit, USU, Upper Sedimentary Unit, PSW, Postavalanche Sedimentary Wedge. Black lines are geological faults. Crossings with other seismic reflection profiles are indicated by line numbers and vertical arrows. Note that only major faults are interpreted; minor faults, especially in the upper part of the margin, have not been the focus of these interpretations. Inferred faults are dashed.

6.1. Raukumara Slump

[25] The Raukumara Slump is best imaged in the Raukumara Basin between 300 and 700 ms below seafloor as a distinctive seismic unit consisting of patches of coherent sediments conformably overlying a high-amplitude, remarkably coherent, subhorizontal basal reflector (Figure 9). The coherent reflections are disrupted by numerous ramps that develop from the basal reflector to create a series of well-defined imbricate structures, with reflection terminations visible at the downslope end. The imbricate structures are observed between ~40 and 110 km north of reentrant wall (northward of CDP 12000 Figure 9), and terminate along a frontal ramp that marks the transition with the otherwise uniform and undeformed sedimentary sequence of the Raukumara Basin (CDP 2100, Figures 9a and 9b). The imbricate structures are therefore buttressed against the undisturbed strata of the Raukumara Basin. The imbricate structures

cumulate an estimated 30% shortening through thrusting and thickening, with a limited amount of displacement in the more distal frontal region. Although the unit is thickened and deformed, the similarity between the stratigraphic sequences across the frontal ramp, together with packages of undeformed sediments conformable with the basin sequence beneath the décollement observed between the imbricate structures, strongly suggests that the imbricate structures consist of remobilized basin sediments with a limited amount of displacement in the frontal region. The geometry and seismic character of the slump are very similar to features described offshore Israel by *Frey-Martinez et al.* [2006], and therefore the unit is interpreted as a frontally confined landslide. Upward, the seismic character of the unit progressively loses coherency and becomes chaotic and featureless, suggesting a different mechanical behavior than at the base of the unit. Although the lateral terminations of the imbricate structures to the east and west are only
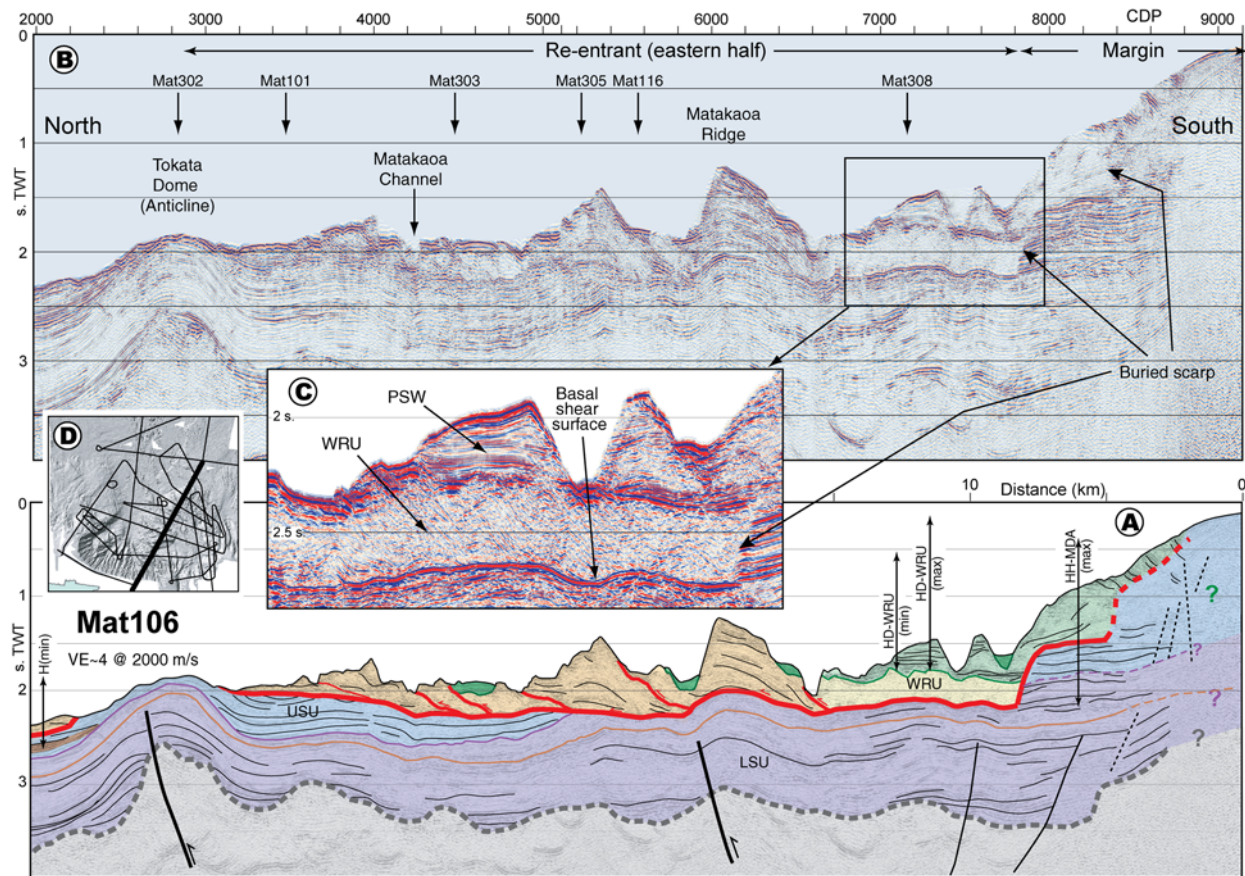
Figure 6. MCS reflection profile Mat106 across the Matakaoa Reentrant. (a) Interpreted profile and (b) uninterpreted processed data. (c) Enlargement on the weakly reflective unit, showing the strong negative reflector indicating the basal shear surface, and the overlying Postavalanche Sedimentary Wedge. (d) Location of profile. See Figure 5 for full caption and color legend and Figure 2 for location of seismic profiles.

constrained by five seismic lines, the observed sharp boundaries of the slump reveal a well constrained area.

[26] Southward along Mat105 and Mat106, the unit thins out, and the basal shear surface onlaps onto the northern flank of the Tokata Anticline (~CDP 2000–2100, Figure 6). Most of the Raukumara Slump is sandwiched within the upper sedimentary unit, which indicates that tectonic deformation continued subsequently to the slumping, as the upper sedimentary unit deposited during tectonic activity. The imbricate structures are identified to the west of the anticline along Mat302 (Figures 8a and 8b). On Mat111, the NW flank of the Tokata Anticline is characterized by a >600-m-thick (650 ms), undulating coherent reflectors overlying a concave-upward basal surface that truncates the coherent well-stratified upper and lower sedimentary units (Mat 111, CDP 2000–4000 Figures 8c and 8d). This facies is interpreted as faulted and back-tilted blocks indicating that the flank of the

anticline has collapsed on a rotational surface, as a slump. This seismic character extends further southward along Mat303 (not shown) and Mat116 (Figure 7), but the coherency of the sedimentary sequence weakens dramatically into a chaotic facies. Beneath the Raukumara Corridor, the basal surface ramps up to the west and truncates the upper and lower sedimentary units in the same manner as on Mat111 (Figures 8c and 8d) and Mat116 (Figure 7), which suggests lateral confinement of the MTD. The upper part of the anticline corresponds to the proximal facies of the slump, whereas the imbricate structures, which it connects with to the north, correspond to the distal part of the deposit. The Raukumara Slump covers an area of ~4000 km² (Table 2 and Figure 11).

6.2. Matakaoa Debris Avalanche

[27] The MDA consists of two remobilized sedimentary masses identified from the seafloor morphology and seismic facies: a weakly reflective

Table 1. Seismic Reflection Character and Relationships With Underlying Units of the Four Mass-Transport Deposits and the Frontal Deformation Zone Forming the Matakaoa Submarine Instability Complex

Name of MTD	Abbrev[a]	Morphology and Seismic Facies	Relation to Underlying Unit	Figure
Turbiditic flow		Very high amplitudes, subhorizontal, extreme coherency and continuity associated with Matakaoa channel. Uppermost unit in reentrant.	Onlapping.	6 and 7
Matakaoa Submarine Instability Complex (MSIC)				
Matakaoa Debris Flow	MDF	Consistent weakly reflective unit with chaotic facies for >180 km. Uppermost unit in Raukumara Basin. Well marked 40-m-high toe at northern end.	High-amplitude, inverse (negative) polarity basal reflector. Truncations.	7 and 10
Raukumara Blocks	-	Hummocky seafloor. Discontinuous from MDF. Internal coherent, high-amplitude reflectors, often tilted.	Embedded in MDF, reaches the MDF basal surface in places.	10
Matakaoa Debris Avalanche (MDA)				
Weakly Reflective Unit	WRU	Coherent, low-amplitude, undulating reflectors + patches of low-frequency, high-amplitude reflectors often tilted upslope.	Highly unconformable on USU and LSU. Basal reflector characterized by high, negative amplitude, and truncations. Onlapping on the blocky unit.	6 and 7
Blocky Unit	BU	Hummocky seafloor, large ridges and hummocks. Blocks and ridges with tilted, high-amplitude, coherent reflectors, lying unconformably over basal negative amplitude reflector. Ridges and hummocks imbricated with contacts merging with basal surface.	Unconformably overlying USU and LSU. Basal reflector characterized by high, negative amplitude, and truncations.	6, 7, and 8
Frontal zone of deformation	FZD	Chaotic reflectors, subhorizontal, imbricated structures merging on a horizontal, high-amplitude coherent reflector. Approximately 200–250 m thick (230 ms).	Highly coherent, high-amplitude basal reflector. Facies is consistent for >30 km.	5 and 9
Raukumara Slump	RS	Distal part: irregular and patchy seismic facies, ~450 ms thick (<500 m); series of flats and ramps over >50 km, with weakly reflective, incoherent cover. Proximal part: highly incoherent facies along the N and NW flank of Tokata Anticline.	High-amplitude, highly coherent, subhorizontal reflectors, gently rising southward (basal surface).	5, 8, and 9
MDA basal shear surface	-	High amplitude, highly coherent and continuous. Negative polarity with respect to the seafloor.	Truncated underlying units (USU and LSU) and onlapping overlying units (WRU, BU).	5 to 8

Table 1. (continued)

Name of MTD	Abbrev[a]	Morphology and Seismic Facies	Relation to Underlying Unit	Figure
Upper sedimentary sequence	USU	Highly coherent, low amplitude subhorizontal beneath continental slope.	Gentle onlaps and truncation in place on USU.	All seismic profs.
Lower sedimentary sequence	LSU	Highly coherent, low amplitude subhorizontal beneath continental slope.	Onlaps on acoustic sedimentary basement.	All seismic profs.

[a] Abbrev: abbreviations used in figures and subsequent tables.

unit essentially occupying the eastern half of the reentrant, and a blocky unit in the centre of the reentrant and its northern approaches. The MDA covers a maximum area of ~1600 km² (Table 2 and Figure 11).

[28] The weakly reflective unit is characterized seismically by coherent, faint, undulating reflectors (Figures 6 and 7 and Table 1) with a maximum thickness of 1 s (800 m). The unit truncates subvertically the continental slope sedimentary sequence beneath the reentrant's southern (CDP7800, Figure 6) and eastern walls (CDP 1400, Figure 7). The conspicuous seismic character of the weakly reflective unit is well recognized on several seismic

profiles in the eastern half of the reentrant, where it shows a maximum thickness of 1000 ms (>900 m). A unit with comparable seismic character, in a similar stratigraphic position and truncating the underlying upper and lower sedimentary units, is recognized beneath the western corner of the reentrant on Mat310 (Figure 10) and Mat308 (not shown [see *Joanne*, 2008]) (Figure 11). However, the lack of traceable correlation between the two units across the centre of the reentrant and beneath the southern wall does not allow us to make an unambiguous connection of the weakly reflective unit over the entire reentrant. This suggests, however, that the weakly reflective unit likely occupies most of the reentrant with a maximum present-day extent of
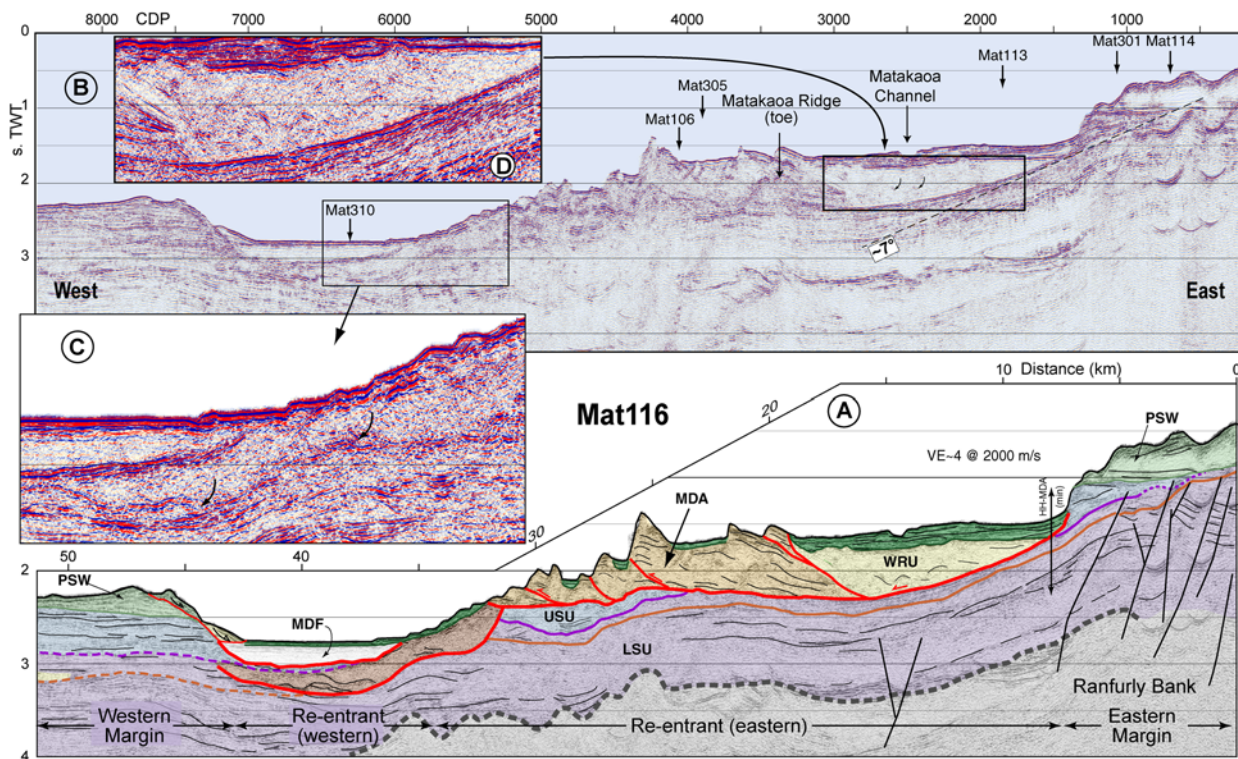

Figure 7. MCS reflection profile Mat116 across the Matakaoa Reentrant. (a) Interpreted profile and (b) uninterpreted processed data. (c) Enlargement on the failed western flank of the Tokata Anticline, and erosional basal surface of the MDF. (d) Enlargement on WRU showing back-tilted reflectors. Curved arrows indicate interpreted back-tilted blocks. See Figure 5 for full caption and color legend and Figure 2 for location of seismic profiles.
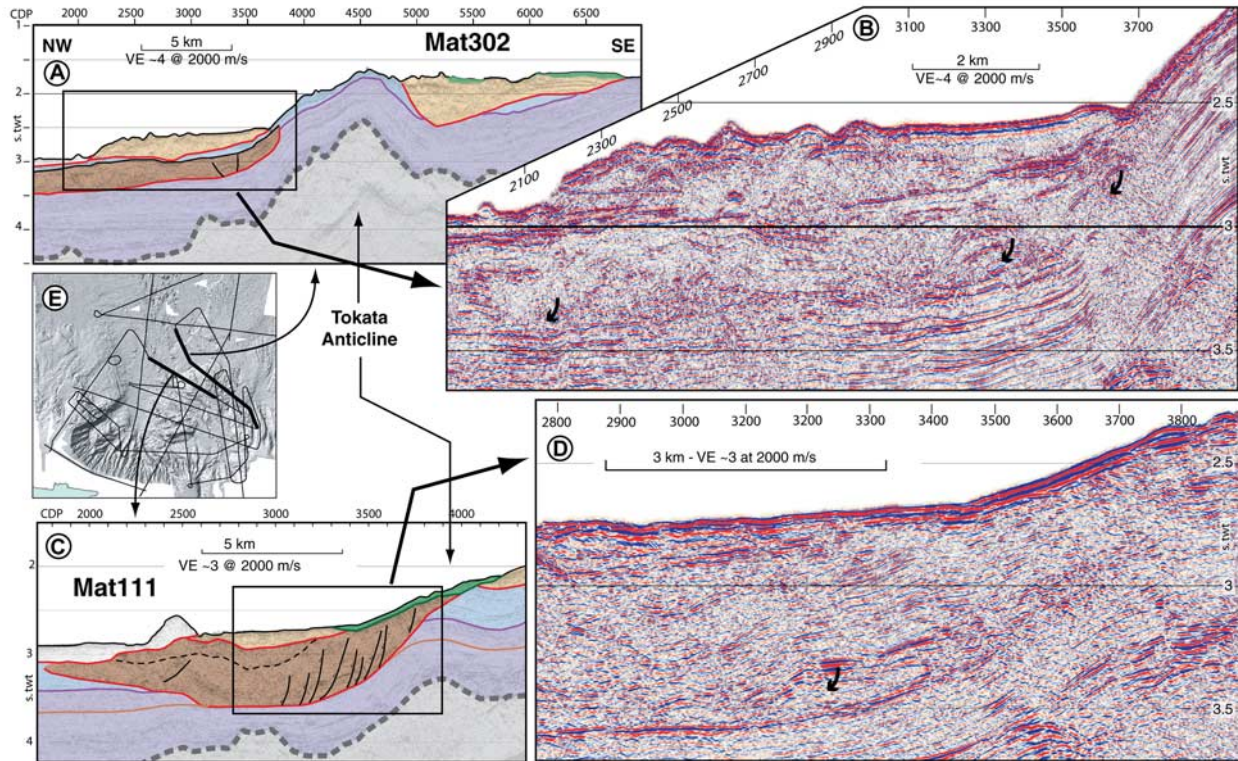
Figure 8. Parts of MCS reflection profiles (a) Mat302 and (c) Mat111 over the NW flank of the Tokata Anticline. Enlargements of uninterpreted seismic reflection profiles (b) Mat302 and (d) Mat111 showing the extension of the Raukumara Slump to the south and the collapsed flank of the anticline. (e) Inset shows the location of seismic profiles. See Figure 5 for full caption and color legend and Figure 2 for location of seismic profiles.

$\sim$460 km^2 (Table 2). A minimum area of 290 km^2 is given by the well defined weakly reflective unit in the eastern half of the reentrant.

[29] The basal surface of the weakly reflective unit is an obvious high-amplitude, negative polarity reflector (Figure 6c) with a concave-upward geometry (Figure 7), which we interpret as the basal shear (or sliding) surface. It dips WNW on Mat116 (Figure 7), and is subhorizontal on Mat106 (Figure 6), which indicates an average NW dip. The basal shear surface connects with the subvertical truncation surface that outcrops at the seafloor in $\sim$800 m water-depth along the reentrant's eastern wall ($\sim$CDP1400, Figure 7), and is buried beneath $\sim$400 m of material along the southern wall (CDP7800, Figure 6). Toplaps immediately beneath the basal shear surface indicate erosion processes. Patches of south dipping coherent reflectors within the weakly reflective unit are interpreted as back-tilted blocks of possibly different rheology (Figure 7a and Line Mat305 (not shown [see *Joanne*, 2008]). The occurrences of back-tilted blocks, together with the rotational basal shear surface, demonstrate the processes of slump emplacement. The basal shear surface extends northward in the centre of the reentrant.

[30] The blocky unit consists of kilometer-wide hummocks, knolls and ridges (Figure 3) which have high-amplitude, well-stratified seismic characteristics. This is best exemplified by the Matakaoa Ridge that culminates $\sim$800 ms ($\sim$800–1000 m) above the basal shear surface (Figures 6 and 7). On Mat116 and Mat106, large blocks have reflectors tilted to the east and south, respectively, which indicate that blocks are back-tilted to the southeast thus corroborating a failure mechanism of a slump. The blocks are arranged in a stacking pattern with northward-verging ramps branching from the basal reflector suggesting a zone of accumulation where blocks are piled up. The basal surface extends further to the east of the Tokata Anticline and to the north into the Raukumara Basin (Figures 5 and 8), where isolated blocks are imaged scattered on the seafloor. Overall the blocky unit covers an area of 1100 km^2 encompassing the eastern half of the reentrant as well as its eastern and northern approaches (Figure 11).
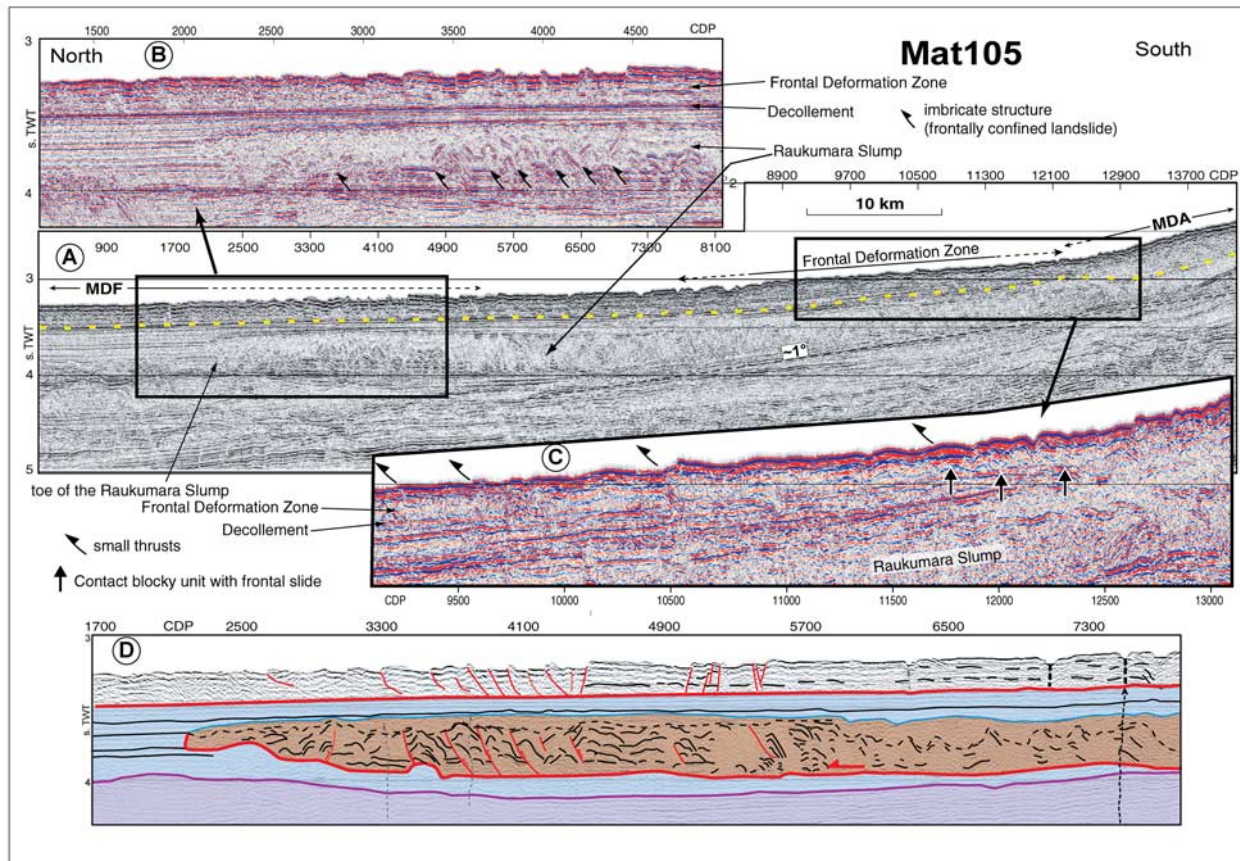
Figure 9. (a) MCS reflection profile Mat105 in the Raukumara Basin, showing the frontally confined landslide associated with the tail end of the Raukumara Slump (see Figure 5 for color legend). Because the line runs very oblique to the transition from the zone of frontal deformation of the Matakaoa Debris Avalanche (MDA) to the Matakaoa Debris Flow (MDF), it is poorly defined on this profile. Lateral erosion of the Raukumara Basin sediments during emplacement of the MDF also contributes to smearing of the transition on seismic profiles. (b) Enlargement of the seismic data over the tail end of the Raukumara Slump. Half-arrows indicate the imbricate structures. (c) Enlargement over the transition from the blocky unit to the zone of frontal deformation. Half-arrows indicate weakly developed thrusts, while black and white arrows indicate the faint transition from the blocky unit to the frontal zone of deformation. Slope gradients are calculated using velocities of 1800 m/s in the upper part of the basin sediment and 2000 m/s in underlying units. Dashed arrows indicate vertical incoherent thin patches across the sedimentary units interpreted as evidence of dewatering. (d) Interpreted section over the tail end of the Raukumara Slump. Color codes and full caption on Figure 5. Location of seismic profiles on Figure 2.

[31] The northern boundary of the blocky unit is interpreted at the slope break (Figure 9a, CDP 12500) that also corresponds with a change from rugged seafloor in the south to smoother seafloor in the north, and appears to be associated with a faint, northward verging reflector (Figure 9, CDP 12000). This geometry implies that the blocky unit slightly ramped over the Raukumara basin sediments near latitude 36°50′S (Figure 11).

[32] Immediately north of the MDA boundary, the seafloor is underlain by weakly deformed basin sediments with patches of high-amplitude, coherent reflectors with a uniform thickness of ∼200 ms

conformably overlying the sedimentary sequence of the Raukumara Basin (Figure 9). The deformation is expressed by small-offset reverse faults, soling out on a 0.5° northward dipping, planar, continuous reflector (Figure 9), corresponding to the basal shear surface of the MDA in the reentrant. The weakly thrust basin sediments, together with the conformity between the reflectors and the basal shear surface, as well as the absence of rotational features within the unit, define a zone of compressional deformation in front of the blocky unit. The deformation is observed for approximately 20 km

Table 2. Morphometric Parameters of the Matakaoa Submarine Instability Complex[a]

| Name | Present Extent, km² | Paleo Extent, km² | Headwall Length, km | | Headwall Height, m | | Runout Dist., km | Height Drop, m | | HD/R Ratio (×100) | | α, deg | |
			HLmin	HLmax	HHmin	HHmax	R	HDmin	HDmax	min	max	min	max
Reentrant	1050		65	90	1450	1750							
MDF	9620	9620	26	43	1200	1900	210	1800[b]	2350	0.8	1.1	0.3	0.5
MDA													
WRU	290–460[c]	290–460[c]	30	52	1100	1600	22	1000	1300	4.6	5.9	2.9	4.2
BU	1100	1345	52	74	1100	1600	65	1800	2100	2.8	3.2	1.0	1.4
FZD	360	500				?							?
RSC	4000	4000[c]	45	55	700	1500	100	1100	1900	1.1	2.0	0.4	1.0
MSIC	13400	13400	37	71	1100	1900	210	1800	2350	1.1	1.3	0.3	0.5

[a] MSIC, Matakaoa Submarine Instability Complex. We estimated the present-day (Present Extent) extents of the remobilized masses and that at the time of emplacement (Paleo Extent). All morphometric parameters are explained on Figure 4c. HD/R is also known as Skempton ratio [*Skempton and Hutchinson*, 1969] (Figure 15).

[b] Minimum height drop calculated assuming a 25% uncertainty on maximum drop.

[c] Minimum area is that identified in the eastern half of the reentrant; maximum area includes a likely continuity with the unit beneath the SW corner of the reentrant (see text and Figure 11).
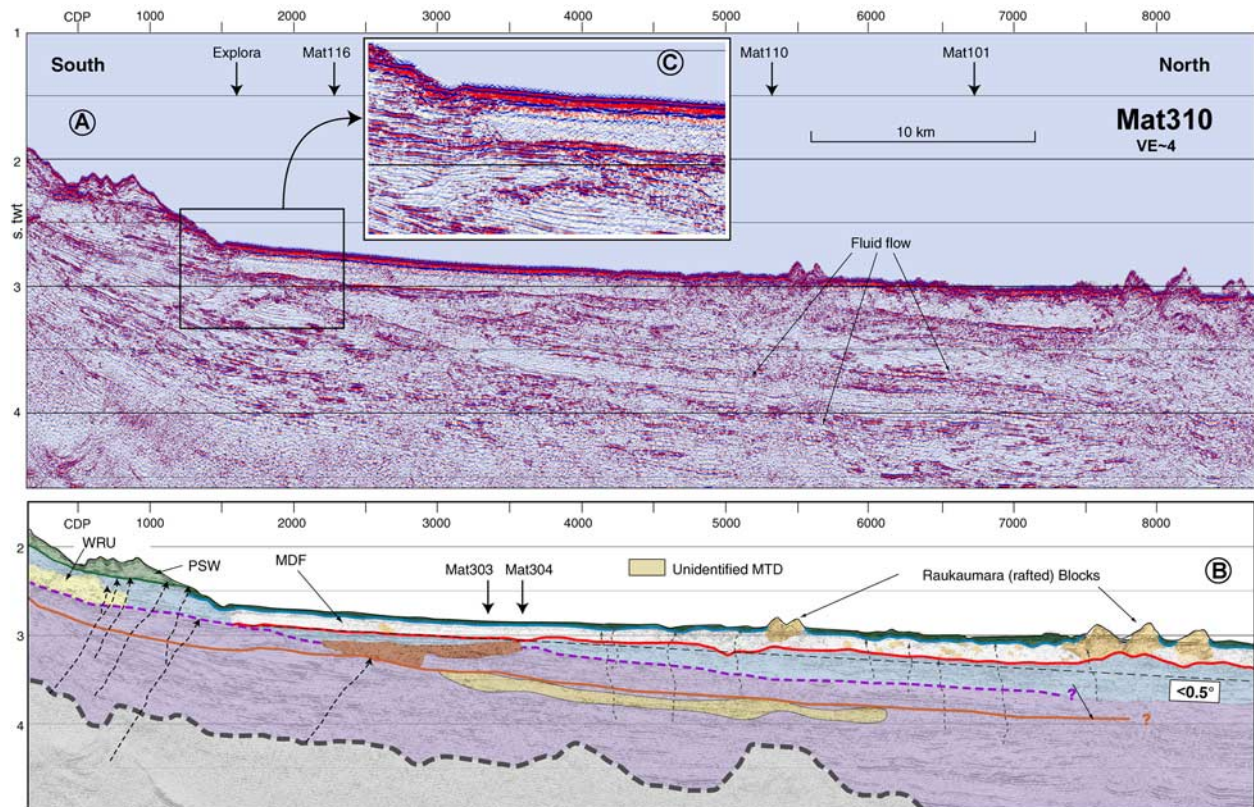

Figure 10. MCS reflection profile Mat310 along the Raukumara Corridor and into the southern part of the Raukumara Basin. The profile shows the Matakaoa Debris Flow (MDF) [*Carter*, 2001] in the upper 250 ms and a series of remobilized units at depth in the basin. Inset shows the base of the MDF with strong scouring of the underlying sedimentary unit. Slope gradient is calculated using a velocity of 1800 m/s in debris flow and 2000 m/s in underlying units. The MTD south of CDP 1000 is interpreted as the westernmost expression of the weakly reflective unit of the Matakaoa Debris Avalanche, but no conclusive ties were found with the facies identified in the eastern half of the reentrant (see text). The dashed arrows indicate vertical incoherent thin patches across the sedimentary sequence interpreted as evidence of dewatering. See Figure 5 for full caption and color legend and Figure 2 for location of seismic profiles.
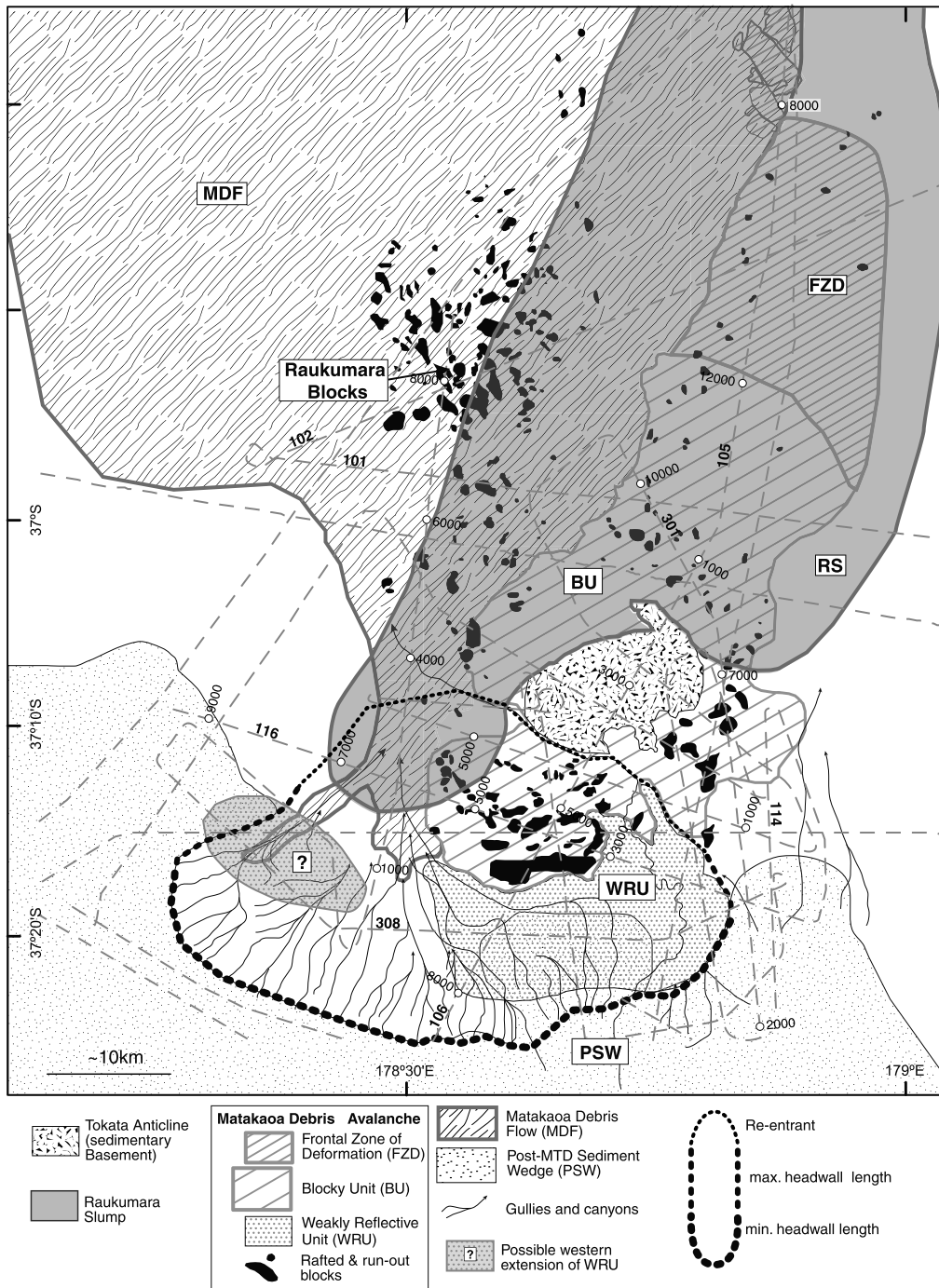
Figure 11. Present-day extents of the mass transport deposits of the Matakaoa Submarine Instability Complex (MSIC), as identified along the Matakaoa Margin and in the Raukumara Basin. Grey dash lines indicate seismic reflection profiles (see Figure 2).

north of the blocky unit (CDP 12000 Figure 9c and Figure 11).

[33] The weakly reflective unit, blocky unit, and the zone of frontal deformation lie on a common shear surface, are continuous in space and overlap each other northward, which together suggest that they formed synchronously. The differing seismic facies imply geologically distinctive components, but the large number of individual blocks identified in the reentrant and in the Raukumara Basin justifies the term "debris avalanche" to describe the deposit complex, in agreement with previous definitions and descriptions of similar features

elsewhere [e.g., *Hampton et al.*, 1996; *Collot et al.*, 2001; *Masson et al.*, 2002].

6.3. Matakaoa Debris Flow and Raukumara Blocks

[34] The Matakaoa Debris Flow (MDF) is characterized by a chaotic, weakly reflective seismic facies and a strongly reflective, basal surface (Mat310, Figure 10) that extends ∼200 km northward of the Matakaoa Reentrant wall. A >40-m-high toe marks the northern termination of the MDF [*Carter*, 2001] (Figure 2b). MDF covers an area of ∼9600 km², has an average thickness of 130 m (Table 2), and a maximum thickness of 340 m (380 ms) in the Raukumara Corridor (Figures 7 and 11). It is covered by a thin veneer (<30 m) of turbiditic and hemipelagic sediments [*Joanne*, 2008].

[35] The basal surface of the MDF truncates underlying strata (Figures 7, 8, and 10c), and at its southern termination, MDF covers a scarp in the continental slope sedimentary unit (CDP1500, Figure 10). The Raukumara Scarp marks the eastern boundary of the MDF, where seismic reflectors within the MDA are truncated (Mat301, Figure 5). The scarp is not connected with geological faults at depth, and is therefore interpreted as an erosion feature. At the toe of the scarp, blocks and ridges that trend parallel to the scarp (e.g., 36°55S, Figure 3) are embedded into the debris flow, suggesting that they detached from the scarp during the emplacement of the flow. The basal truncation surface, together with the buried scarp to the south, and the Raukumara Scarp to the east imply that the MDF eroded the preexisting sedimentary sequence during its emplacement.

[36] The Raukumara Blocks consist of individual kilometer-long blocks with internal stratification. The block bases either correspond with or are shallower than the MDF basal surface (Figures 2 and 10), with evidence, albeit weak, of debris flow material between the basal surface and the blocks (e.g., line Mat 310, Figure 10). In map view, the pear-shaped distribution of the Raukumara Blocks points southward, suggesting the blocks originated from the centre of the reentrant (Figure 2).

7. Age Control

[37] Core #10 acquired during the 2001 voyage of R/V *Tangaora* is a 2.76-m-long gravity core recovered in a 85- to 115-m-thick sediment-ponded basin on the MDA in the centre of the reentrant (location on Figure 2). Core #10 consists of silty to clayey hemipelagic sediments with thin interbedded turbidites and tephra layers, which we consider as representative of the postavalanche sedimentation. Tephrochronology, carbonate content and stable isotope analyses allow us to develop a multiproxy age model for the timing of avalanche emplacement (Figure 12). Glass shards in two macroscopic tephra layers at 70 cm and 226 cm depth are chemically finger-printed to the 5.5 ka Whakatane, and 13.7 ka Waiohau volcanic eruptions, respectively [*Lowe et al.*, 2008], in agreement with the placement of the Marine Isotope Stage (MIS) 1/2 boundary close to 220 cm based on the $\delta^{18}O$ isotope curves. From these results, a postglacial sedimentation rate of ∼0.17 ± 0.02 mm/a can be estimated. As a first approximation, and using this sedimentation rate since emplacement of the MDA, we derive an age of 600 ± 150 ka for the mass failure. We believe that this represents a maximum age, because of the likelihood for increased sediment supply during glacial periods, as noted on the nearby east coast margin [*Carter and McCave*, 2002; *Collot et al.*, 2001; *Lewis et al.*, 2004]. Furthermore, turbidites deposited in the reentrant could give erroneous sedimentation rates using the simple model presented above. As a matter of comparison, *Orpin et al.* [2006] give sedimentation rates of 1 mm/a in slope basins and 0.5 mm/a for the Holocene, along the Hikurangi Margin, 120 km south of East Cape, in a region with lower sediment supply than that of the Waiapu River. Such sedimentation rates would result in an age potentially as young as 120 ka for the emplacement of the MDA. This absolute minimum age of 120 ka suggests a possible synchronicity of occurrence of the MDA and the Ruatoria Avalanche, which if verified would imply a relationship between the triggering of both events, and have implications on the immediate geomorphological response of the margin to two giant submarine mass failures.

[38] We have no further constraints on the age of the Matakaoa Debris Flow than that provided by *Carter* [2001], who based his estimate of 38–100 ka from a core collected in the Raukumara Basin, 16 m above the top of the debris flow and a 0.13 mm/a sedimentation rate derived from a core collected on the continental slope.

[39] We assume a Pleistocene age for the Postavalanche Sediment Wedge deposited within and on both sides of the reentrant. In the reentrant, the sediments deposited over the MDA headwall lie unconformably on the weakly reflective unit, and
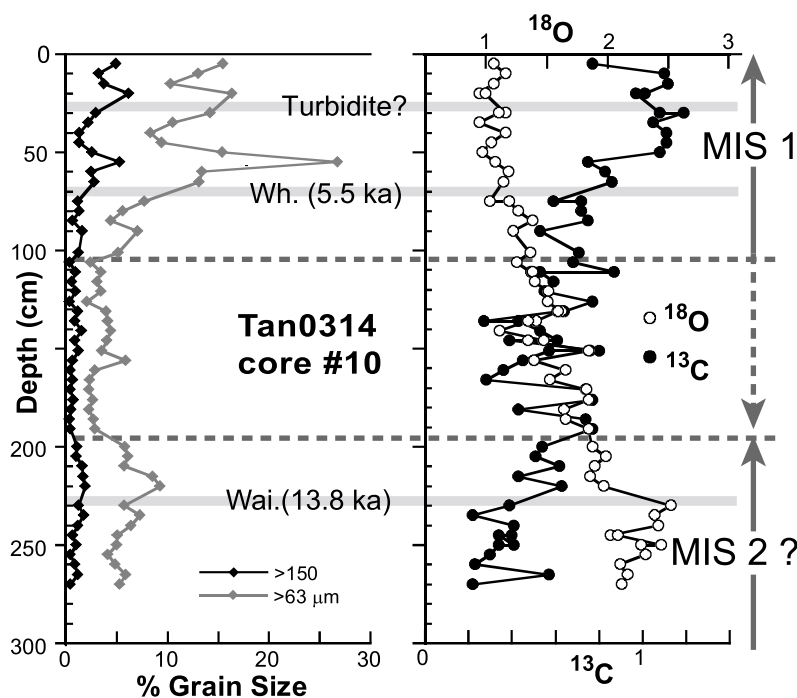
Figure 12. Multiproxy age model for the emplacement of the Matakaoa Debris Avalanche, including variations in carbonate content and $\delta^{18}O$ isotope in core #10. Tephra layers are identified as the Whakatane (Wh) and Waiohau (Wai) events at 70 and 226 cm, respectively. Ages of the volcanic events are indicated. All values of isotope analysis are relative to vPDB, where $\delta^{13}C$ and $\delta^{18}O$ have values of +1.95‰ and −2.20‰ for NBS19 calcite, respectively. Samples were analyzed using an individual-carbonate reaction (Kiel) device coupled with a Finnigan MAT252 mass spectrometer. The transition from Marine Isotope Stage (MIS) 1 to 2 is interpreted at ∼220 m (thick dotted grey line), and a less likely alterative is interpreted at ∼100 cm.

were therefore deposited after the emplacement of the MDA, i.e., since mid to upper Pleistocene.

[40] An unconstrained Pliocene age for the emplacement of the Raukumara Slump can be derived from the 350- to 400-m-thick sedimentary sequence observed above the slump in the Raukumara Basin, using estimated Pleistocene sedimentation rates ranging from 0.1 to 0.7 mm/a [e.g., *Carter*, 2001; *Collot et al.*, 2001], because geologically older sedimentation rates are not known from the basin. Long piston cores acquired in January 2006 in the Raukumara Basin may help better constrain the age of the slump [*Proust et al.*, 2006].

8. Discussion

[41] Because the MSIC includes slumps, debris avalanche and debris flows, it is best described as a submarine instability deposit complex. In order to propose a semiquantitative scenario of the modes of emplacement within the MSIC, we combine results from the age model developed above with estimates of remobilized volumes, together with interpretations of the geographical and stratigraphic

origins of each component of the deposit complex. This approach allows us to clarify the mechanisms of failure and transport processes involved during different phases of MSIC emplacement.

8.1. Origin and Transport of MSIC Deposits

8.1.1. Raukumara Slump

[42] We interpret the imbricate structures in the Raukumara Basin as a frontally confined landslide representing the distal part of the Raukumara Slump, and the collapsed NW flank of the Tokata Anticline as a portion of the proximal part of the slump.

[43] The imbricate structures clearly indicate compressional deformation and displacement of competent sediments on a single décollement. The more chaotic and weakly reflective seismic facies overlying the imbricate structures (Figure 9) suggests material of different rheology and mechanical behavior. The gradual transition from the imbricate structures to the chaotic seismic facies indicates a common origin. The facies of the superficial layer

possibly reflects the lower shear strength of poorly consolidated sediments, submitted to mass transport.

[44] Assuming that the toe of the slump is pinned as a no-deformation point, unfolding by 30% the imbricate structures suggests that the deformed sediments could not originate from as far south as the present-day reentrant headwall, and that the material involved in the imbricate structures does not originate from the reentrant.

[45] The proximal part, which relates to the slump depletion zone, is difficult to identify for two main reasons; first, because the MDA postdates the Raukumara Slump and therefore substantial parts of the scar and material have been eroded by the MDA (Figure 13, T3); and second, because folding continued after deposition of the upper sedimentary unit so that the present-day slope of the western flank of the Tokata anticline is not necessarily representative of the geometry of the margin at the time the emplacement of the slump, during the Pliocene.

[46] However, we recognize the imbricate structures as far south as Mat302 and a segment of the rotational basal surface of the slump farther south on Mat111 (Figures 8 and 11). These structures suggest that the slump scar and depletion zone were located in the close vicinity of the Tokata anticline. Furthermore, the slump mass is interpreted beneath the Raukumara Corridor as far south as Mat116 indicating that the slump may have originated from farther south than the Tokata anticline. The very narrow width (~12 km) of the slump in the Raukumara Corridor (Figure 11) contrasts with the ~35 km width to the north, suggesting that the depletion zone was likely larger than that interpreted in the southernmost part of the slump (Figure 13, T1).

[47] Hence we propose that the Raukumara Slump initiated within the northern half of the reentrant by the failure and slip of the Raukumara Basin sedimentary sequence that propagated northward, thus forming the distal imbricate structures (Figure 13, T1). Because of the MDA, the depletion zone was partially destroyed.

8.1.2. Matakaoa Debris Avalanche

[48] The MDA consists of two remobilized units emplaced synchronously: the weakly reflective unit and the blocky unit. Reconstruction of the geometry of the basal shear surface indicates it dips NW beneath the eastern part of the reentrant (Figure 14), and connects southward and southeastward with the

avalanche headwalls. The nature of the basal shear surface varies laterally. Within the reentrant, the shear surface lies conformably over the NW dipping stratigraphic sequence (Mat116, Figure 7), and is therefore interpreted as a décollement, whereas it is a truncation surface beneath the headwall. The shear surface projects beneath the margin along the unconformity between the upper to lower sedimentary units, suggesting this stratigraphic layer acted as a weakness plane along which the failure initiated and propagated. This evidence, together with the occurrence of back-tilted blocks in both the weakly reflective and blocky units, suggest that the margin failure process was that of a slump originating from the SE corner of the reentrant, and that the slump formed a debris avalanche deposit. The well marked scarp in the southeast corner of the reentrant (Figure 3) can therefore be interpreted as the origin of the Matakaoa Ridge, which indicates that the ridge slid ~15 km along the basal shear surface.

[49] The MDA remobilized material of different rheologies, all originating from within the Matakaoa Margin. On the continental shelf, the deformed sedimentary basement and the overlying shelf basins have distinctive seismic characteristics [Lewis et al., 2004]. The sedimentary basement has a well-stratified, high-amplitude seismic character, associated with Mio-Pliocene indurated sediments, whereas the shelf-basin reveals weaker reflectivity associated with Quaternary sediments, probably with higher porosity and water content. These seismic characters closely resemble those of the blocky and weakly reflective units. The relative geographic positions of the two remobilized units, i.e., the weakly reflective unit upslope and the blocky unit downslope, corroborate our interpretation that the blocky unit represents an original basement high on the edge of the continental shelf. Failure of the basement high along Ranfurly Bank released the Quaternary sediments trapped in a shelf basin, similar to the modern Waiapu or Te Aroha basins (Figures 1 and 2), thus forming the weakly reflective unit.

[50] The tectonic activity associated with the Pacific-Australia convergent plate boundary is likely to have played a major role in generating repetitive slope instabilities in the region. Margins with seaward dipping strata, like the Matakaoa Margin, naturally offer weakness planes where dip-slip may require less energy to initiate failure than those with landward dipping strata. Along the Matakaoa Margin, compressional tectonics further increased the seaward dip of the strata (7–10°, Figure 7)
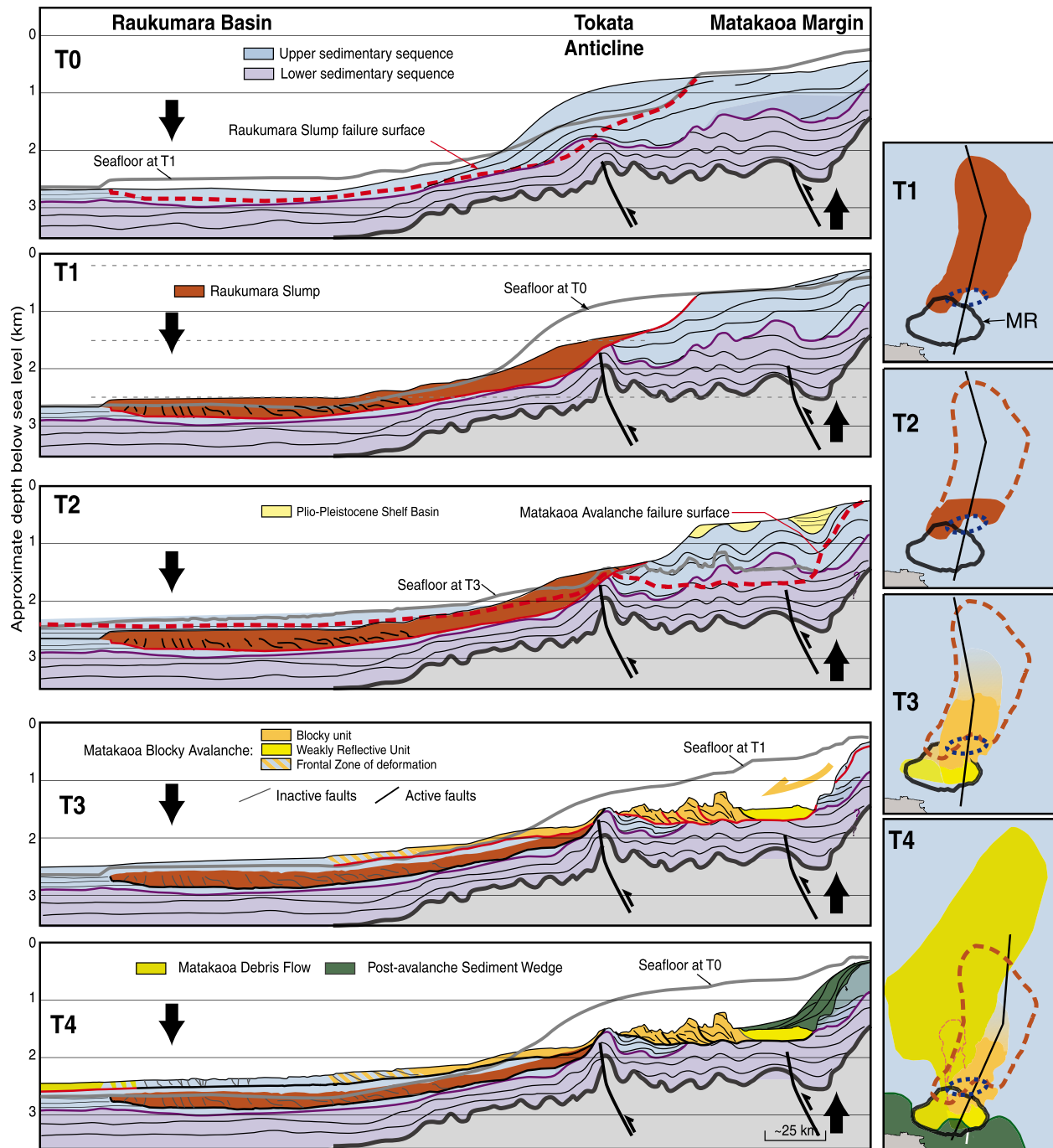
Figure 13. Sketches of the scenario for the implementation of the Matakaoa Submarine Instability Complex. Estimates of timing (see text) are T0, Mio-Pliocene; T1, Pliocene; T2, Plio-Pleistocene; T3, 600 ± 150 ka; and T4, $100 - 38$ ka. The maps on the right side show the extents of the MTDs immediately after emplacement. Straight lines are approximate locations of the cross-section sketches. Dashed lines indicate paleo extent. Dashed blue lines (ellipsoid) indicate the location of Tokata Anticline. The thick black line indicates extent of the Matakaoa Reentrant (MR). Thick vertical arrows suggest uplift and subsidence.

compared with the average seafloor slope of $3-4°$ westward of the reentrant (Figure 4a). The combination of high Quaternary uplift rates [*Wilson et al.*, 2007b] and the inferred subsidence in the Rauku-

mara Basin, resulted in the continuous northward tilting of the north dipping continental slope. Therefore uplift and compressional tectonics are considered to be a major factor of slope instability in the
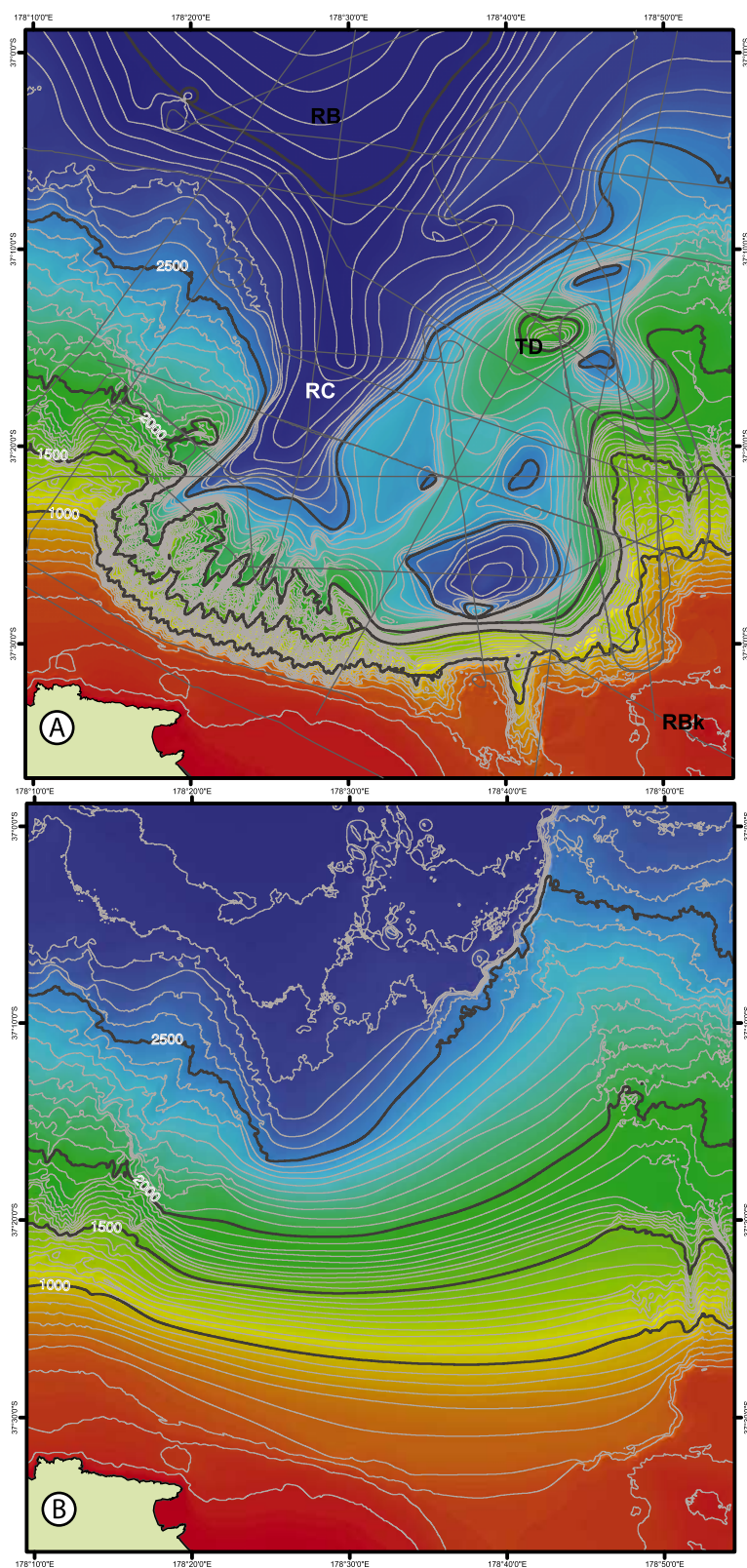
Figure 14

region, since at least the upper Miocene. Variations in uplift rates may have also contributed to the recurrence of large slope instabilities.

[51] The compressional regional tectonic activity has further consequences on the subsequent transport and deposition of the MDA. In particular, the deformation associated with the Tokata Anticline has clearly impacted on the spatial arrangement of the MDA. The rafted blocks to the south and east of the Tokata Anticline demonstrate that the anticline deflected the MDA during its emplacement, and resulted in the concentration of the largest blocks (i.e., the Matakaoa Ridge) in the proximal region within the reentrant. It has been recognized that large rafted blocks often acquire the maximum kinetic energy and consequently travel farthest [*Collot et al.*, 2001; *Haflidason et al.*, 2005; *Hampton et al.*, 1996]. In the MDA, the blocks stacked up against each others because they were restrained from sliding further north by the Tokata Anticline that acted as a natural dam. This stacking pattern necessarily required high transport energy, and indicates that the blocks failed catastrophically.

[52] In its most distal part, the MDA destabilized the recent sedimentary sequence of the Raukumara Basin and formed a zone of compressional deformation in front of the blocky unit for approximately 20 km. The minor thrusts resulted in small offsets in the sedimentary sequence associated with low seafloor reliefs, which indicates a small amount of displacement over the planar basal shear surface. The relative preservation of the basin stratigraphy in the frontal deformation zone, conformably overlying the Raukumara Basin sequence, together with patches of continuous and high-amplitude reflectors argue against this zone being interpreted as a debris flow. The overlapping contact between the blocky unit and the frontal zone of deformation (CDP12500, Figure 9c), which have a common sliding surface, suggests that the compression resulted from stress transfer from the toe of the blocky unit to the basin sediments.

8.1.3. Matakaoa Debris Flow

[53] The MDF originated from the western part of the reentrant [*Carter*, 2001], and left a 1100-m-high scarp implying high potential energy of the original failure. The 200 km runout distance of the MDF on very gentle slope gradient (<1° and down to 0.05° at deposition) suggests high mobility [*De Blasio et al.*, 2006]. Long runout distances are suggestive of either high fluid content or a relatively low clay/sand ratio (0.2 to 0.3) [*Ilstad et al.*, 2004], as both conditions result in low yield strength, which favors mobility and high speed of the flow [e.g., *De Blasio et al.*, 2006; *Marr et al.*, 2001].

[54] The flow shows evidence of powerful basal and lateral erosion. Basal erosion is particularly well imaged within, and immediately north of, the Raukumara Corridor, where the flow truncates the underlying sedimentary units (Figure 10). We suggest that the Raukumara Scarp formed by lateral erosion of MDA and basin sediments by the MDF. Powerful erosion is more likely to occur in association with strongly coherent debris-flows [*Marr et al.*, 2001; *Mohrig et al.*, 1999]. The debris flow's maximum energy occurred at the base of the continental slope where the potential energy was converted into kinetic energy. The maximum energy of the flow was possibly increased through the constriction of the debris flow in the Raukumara Corridor, thus accounting for more significant erosion in the proximal region of the flow.

[55] In the Raukumara Basin, the pear-shaped distribution of the Raukumara Blocks in map view (Figures 3 and 11) suggests that they were remobilized from the western edge of the MDA in the reentrant and transported with the MDF during its emplacement. This would have required substantial erosional energy from the debris flow during transport.

8.2. Volume Budget

[56] Sediment budgets require balancing volumes or masses of solid particles because the total

Figure 14. Reconstructed topography of the Matakaoa Margin. (a) Topography with all material above the basal shear surface of the MDA and MDF removed using an average velocity of 2000 m/s. Subtraction of both DTMs using GIS software provides a volume of material removed of 1300 km³. TD, Tokata Dome (the morphological expression of the Tokata Anticline); RC, Raukumara Corridor; RBk, Ranfurly Bank; RB, Raukumara Basin. (b) Interpreted margin topography before failure of the Matakaoa Debris Avalanche and creation of the reentrant. The contour lines were extended from either side of the indentation, assuming the Tokata Anticline was outcropping at the seafloor at the time. Seismic lines are shown in light grey and give an indication of the constraints available for interpreting the paleotopography.

volume of solids involved in a slope failure is conservative, rather than the bulk volumes that include pore space and therefore are inherently variable. Establishing a sediment budget is a prerequisite to propose a scenario for the emplacement of any MTD. Here, we differentiate bulk and compacted volumes, in a similar manner as *Collot et al.* [2001]. Bulk volumes correspond to the amount of displaced material observed today, whereas volume of solid are compacted to a theoretical zero-porosity. Because debris flow and margin rocks have different porosities, we calculated their compacted volumes of solid to perform valid comparisons between missing and redeposited volumes. This requires that we also calculate the "empty" volumes of the reentrant to the equivalent volume of solid of prefailure margin sediments. This does not imply, however, that the porosity of the material prior to failure was zero. Rather, compacted volumes are independent of the margin ages and composition, and therefore enable more robust comparisons of remobilized masses globally.

[57] The Raukumara Slump has an estimated total bulk volume of 1400 ± 360 km^3 (Table 3). Because part of the Raukumara Slump deposited in the reentrant has most likely been remobilized by subsequent events, in particular during the deposition of the MDA, our volume estimate is underestimated.

[58] The MDA has a total bulk volume of 430 ± 100 km^3, subdivided into 260 ± 50 km^3 for the blocky unit and 170 ± 50 km^3 for the weakly reflective unit (Table 3). The frontal zone of deformation represents an estimated 120 ± 25 km^3 of material. Presently, the NW boundary of the MDA corresponds with the Raukumara Scarp. As the scarp resulted from lateral erosion, the original area covered by the MDA was larger than that observed today. We estimate the original extent of the MDA immediately after failure, from an "ideal" symmetrical lobate shape including detached blocks accumulated at the base of the Raukumara Scarp (Tables 2 and 4, Figures 11 and 13).

[59] A bulk volume of 1250 ± 250 km^3 was calculated for the Matakaoa Debris Flow using an average thickness of 130 m and a total area of 9620 km^2. Because the debris flow is superficial and shows no evidence of erosion subsequent to its emplacement, we believe its present-day extent is comparable to its original (Table 2) and that the uncertainty on the area is 10%. However, the volume of material that originally failed from the margin is likely to be overestimated as the debris flow shows widespread

evidence of extra material being incorporated to the mass through basal and lateral erosion during emplacement. We calculated the amount of material potentially added to the MDF volume through accretion by estimating the thickness of material eroded from the upper Raukumara Basin sedimentary sequence at the base of the flow, and the difference between the present-day and the paleo extents of the zone of frontal deformation as estimated from an assumed ideal lobate shape (Table 4). This suggests that approximately 30% of the bulk volume of the debris flow could have been added by accretion. Despite being one of largest debris flow worldwide, the very long run out distance of the MDF results in a low Skempton ratio [*Skempton and Hutchinson*, 1969] (HD/R, where HD is total height and R is runout distance) of ~0.01 (Table 2), and when positioned on a HD/R versus volume diagram the MDF compares well with other slides and debris flows globally for submarine mass movements (Figure 15) [*Hampton et al.*, 1996; *Canals et al.*, 2004].

[60] A volume of 1300 ± 260 km^3, similar to that estimated by *Carter* [2001], is calculated for the reentrant, representing the amount of material between the reconstructed topography of the margin prior to failure and the MDA basal shear surface (Figure 14).

[61] We use the porosity values given by *Collot et al.* [2001] to calculate the volumes of solid of each component of the MSIC (Table 3). This is justified because the Matakaoa Margin is only 40 km NW of the Ruatoria Avalanche head-scarp and has remobilized similar geological material from the continental margin. The compacted volume of the Raukumara Slump is estimated to be 1150 ± 340 km^3. For the MDA, the compacted volumes are 210 ± 60 km^3 for the blocky unit and 70 ± 20 km^3 for the weakly reflective unit. We further estimate a 500 ± 150 km^3 volume of solid for the MDF. Following on the previous section, we believe that up to 30% of the compacted volume of the MDF could have been added to the original failed mass, through basal scouring and lateral erosion (Table 4). Hence, the compacted volume of material failed from the continental slope during emplacement of the MDF could be as low as 350 km^3, whereas the solid volume of the empty reentrant (i.e., the volume occupied by the MTDs before failure) is estimated to be 1100 ± 330 km^3. While the bulk volume of the MDF is of similar magnitude to that of the reentrant, we believe the failure of the MDF alone cannot have produced the

Table 3. Volumes Calculated for the Matakaoa Submarine Instability Complex and the Matakaoa Reentrant[a]

Name	Vel., m/s	Av. Thick. (h), m	Max Thick. (hmax), m	Method	Bulk Vol., km³		A/V^{2/3}	Por.	Compacted Vol., km³		V^{2/3}	A/V^{2/3}
Matakaoa Reentrant	2000	-	-	1	1300	±260	9	15%	1110	±330	107	10
MDA												
Weakly Reflective Unit	1800	-	900	2	170	±50	13	60%	70	±20	17	28
Blocky Unit	2000	-	-	1,2	260	±50	33	20%	210	±60	35	31
Frontal zone of deformation	2000	225	275	3	120	±25		20%	90	±20		
Matakaoa Debris Flow	1800	130	230	3	1250	±250	83	60%	500	± 150	63	153
Raukumara Slump	2000	360	750	2,3	1400	±360	31	20%	1150	± 340	110	36
Matakaoa Submarine Instability Complex					3200	±640	62		2020	± 600	160	84

[a] Velocities (Vel.) are P wave velocities used for time-to-depth conversions in the estimation of maximum (Max) and average (Av.) thickness of remobilized masses. Bulk Vol. is present-day bulk volume of the remobilized masses without compaction of material. Method is that used to calculate the bulk volumes: (1) Subtraction of upper and lower reconstructed surfaces from Digital Terrain Models (DTMs) generated from interpretation of seismic profiles and multibeam bathymetry (Figure 14). (2) Remobilized mass is divided in polygons of regular thickness; volume calculated as the sum of individual polygon volumes. (3) Product of the average thickness of remobilized masses by paleo extents (Table 2). We used the estimated extent of the remobilized masses at the time of implementation, i.e., before any subsequent erosion occurs. Por. is estimated porosity used to calculate the compacted volumes of solid [from *Collot et al.*, 2001]. Compacted Vol. are calculated as Bulk Volume*(100-Porosity)/100. The "empty volume" of the reentrant is also compacted to an equivalent volume of solid of margin material for valid volume budget. See Figure 4c for explanation of h and hmax. A/V^{2/3} is used to estimate the flow efficiency of slides [*Dade and Huppert*, 1998; *Haflidason et al.*, 2005]. A minimum error of 20% in the volume calculations is estimated as the sum of uncertainties of velocities (10%) and seismic interpretation errors (10%). A 30% error is estimated for the compacted volume. Abbreviations spelled out in Table 1.

reentrant since their compacted volumes are significantly different.

[62] We do not include the volumes of the frontal zone of deformation and Raukumara Slump in the comparison with the empty volume of the reentrant as the former represents material of the Raukumara Basin, and the part of the latter that originates from the reentrant is unknown. We note however that a subdued reentrant may have remained following the failure of the Raukumara Slump as suggested by the reconstruction of the margin topography prior to the failure of the MDA (Figure 14). Together, the weakly reflective and blocky units of the MDA and the MDF represent a bulk volume of 1680 ± 350 km³ and a compacted volume of 780 ± 260 km³ (Table 3). The cumulative bulk volume of remobilized material originating from the reentrant (1680 km³) is therefore markedly larger than the bulk volume of the reentrant (1300 km³), while the compacted volume (630 km³) is markedly smaller than that of the reentrant (1100 km³). It is unlikely that the blocky and weakly reflective units of the MDA alone represent the entire content of the reentrant, since their compacted volume (280 km³) is conclusively smaller than the volume of the reentrant (1100 km³). Post-failure processes of retrogressive erosion associated with the activity of slope-confined canyons must have played an important part in the excavation of the reentrant [*Joanne*, 2008]. We also believe that the discrepancy between the compacted volumes of the reentrant and that of MDF+MDA confirms that an indentation was created in the margin by the

Table 4. Estimate of Material Added to Matakaoa Debris Flow During Emplacement Through Basal Scouring and Lateral Erosion[a]

	Extent, km²	Av. Thickness, m	N	Min-Max, km²	Average, km²	Cumulated Area, km²	Vol., km³	Compacted Vol., km³	Vol./Vol. MDF	Vol./Vol. MDF Compacted
Raukumara Blocks	490 ± 20	170	76	0.1–4.5	0.8	58 ± 12	10	8.5	1%	2%
FZD + Raukumara Basin Sediment	640 ± 100	250	-	-	-	-	160	128	13%	26%
Basal erosion	120	20	-	-	-	-	20	12	2%	2%
Total							190	148.5	16%	30%

[a] Extent of Raukumara blocks is the cumulated area of individual blocks (Figure 2). We use the same method as in Table 3 to calculate the compacted volumes of solid. The ratios of the eroded volumes over that of the MDF are given in the last two columns. A total of up to 30% of the compacted volume of the MDF (Table 3) may have been added during emplacement.
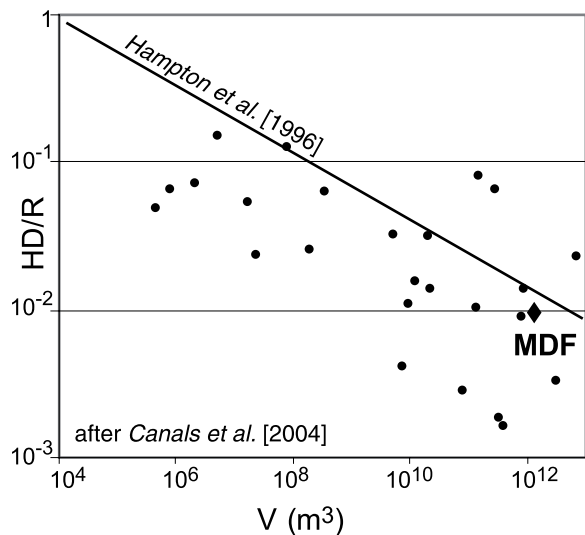
Figure 15. Skempton ratio (total drop (HD) over runout distance (R)) as a function of volume for the Matakaoa Debris Flow (MDF) superimposed on a global data set for large MTDs from *Canals et al.* [2004] and upper bound for submarine landslides (black line) from *Hampton et al.* [1996]. See Figure 4d for explanation of HD and R.

Raukumara Slump and had not been completely filled before the failing of the MDA.

8.3. Sediment Loading From the Waiapu River as Factor of Slope Instability

[63] One of the most remarkable characteristics of the sedimentary environment of the East Cape region is the very high supply delivered from the local rivers. It is therefore important to evaluate the significance of this high sedimentation supply on the recurrence of large mass failures, which include the Ruatoria avalanche and MSIC, to the east and north of East Cape, respectively. The Waiapu River alone discharges an average of 36×10^6 t of sediment per year on the continental shelf and slope. The Motu River, on the west coast of the Raukumara Peninsula delivers an estimated 3.5×10^6 t of sediment per year on the continental shelf [*Hicks and Shankar*, 2003]. Currents offshore and inshore of the 1000 m isobath flow in opposite directions [*Carter*, 2001; *Carter and McCave*, 2002; *Chiswell and Roemmich*, 1998] so that both rivers could contribute to sediment accumulation over the Matakaoa Margin. These values are all postdeforestation subsequent to human settlement in New Zealand and therefore largely exceed the average sediment discharge for the Holocene. *Orpin et al.* [2006] estimate that the total sediment budget for

the Holocene in the Poverty Bay region, ~120 km south of East Cape, is ~1×10^6 t/a, and *Lewis et al.* [2004] mapped thick accumulation of post–last glacial sediments in the Waiapu shelf basin (Figure 1). At the shelf break, slumping and hyperpycnal deposition of river sediments attest to the high instability of the recent sediment [*Lewis et al.*, 2004]. Hyperpycnal flows are guided by subtle shelf relief into the Matakaoa Channel to the north and similar well defined channels on the Hikurangi Margin to the east, thus transporting sediments into basins that are forming behind blocks of the Matakaoa and Ruatoria avalanches. We infer that the Waiapu River contributes to the source regions of both Matakaoa and Ruatoria avalanche complexes during highstands, but the MSIC may be the preferred depocenter during lowstands judging by the presence of a canyon head that incises the headwall scarp (Figures 2 and 3). However, because there is no published sedimentation rate for the Pleistocene, we used a constant Holocene sedimentation rate to estimate the age of the MDA, which results in a large uncertainty and prevents from relating the MDA event to the eustatic cycles. The high supply of sediment from local rivers may contribute to healing mass-failure scars by rapidly reconstructing the margin sedimentary architecture, thus preparing for the next major failure. Further mass balance relating river inputs to prefailure sediment volumes may help constrain the minimum recurrence of large failures.

8.4. Scenario of MSIC Emplacement

[64] The spatial organization of the four remobilized masses that constitute the MSIC, together with the age model developed in this study are used to propose a relative chronology of the events and a scenario of the modes of implementation of the MSIC in five stages T0 to T4 (Figure 13, T0 to T4).

[65] T0 (Mio-Pliocene), is a period of continental slope and basin sedimentation across the Matakaoa Margin and in the Raukumara Basin which preceded the emplacement of the Raukumara Slump. The region was under a compressional tectonic regime which resulted in the folding and faulting of the sedimentary sequence beneath the continental slope, but the Tokata Anticline remained a subdued structural and topographic feature at this stage. The continental slope was located up to 30 km north of the present reentrant headwall and its toe corresponded to the northern flank of the Tokata Anticline.

[66] At T1 (Pliocene), the failure of the upper part of the continental slope as the Raukumara Slump, was likely related to tectonic activity as indicated by the then growing Tokata anticline and the failure of its north-western flank. The Raukumara Slump remobilized material for > than 50 km into the Raukumara Basin and terminated against the otherwise gentle basin sedimentary sequence as a frontally confined landslide.

[67] T2 (Plio-Pleistocene), corresponds to a period of hemipelagic and turbiditic sedimentation in the Raukumara Basin and over the continental slope. Sedimentation on the continental slope partly healed the scarp formed during the emplacement of the Raukumara Slump. Continuing regional compressional deformation resulted in further faulting and tilting of sedimentary basement blocks on the continental shelf and in the growth of the Tokata Anticline as a prominent morphological feature. The combined effect of uplift of the Raukumara Peninsula and Ranfurly Bank and subsidence in the Raukumara Basin resulted in a continuous increase of the north-westward dip of the continental slope. High terrestrial sedimentation generated from high onland erosion filled shelf and slope basins.

[68] At T3 (600 ± 150 ka) the emplacement of the Matakaoa Debris Avalanche followed the collapse of a kilometer-wide Mio-Pliocene sedimentary basement block at the edge of the continental shelf as a large slump that also released the Plio-Pleistocene sediment infills of the shelf basins. The indurated Mio-Pliocene sediments were transported as a series of blocks that piled up against the buttress formed by the outcropping Tokata Anticline. The younger, less compacted shelf-basin sediments filled the depression left by the slumped material. The distal part of the MDA was deflected northward around the Tokata Anticline, and destabilized the superficial sediments of the Raukumara Basin deposited over the northern flank of the anticline over a distance of ~20 km.

[69] At T4 (100-38 ka), the sediment accumulated in the western part of the reentrant during the Pleistocene failed and formed the Matakaoa Debris Flow (MDF). The Raukumara Corridor guided the MDF toward the Raukumara Basin, and during its emplacement the MDF eroded part of the MDA to form the Raukumara Scarp.

[70] Continued sedimentation from high-yield rivers since deposition of the MDF contributed to the gradual healing of the reentrant, but also led to the delivery of unstable material that has built into the continental slope. Today, a turbidite plain is developing in the eastern part of the reentrant and a channel is forming as a result of continuous sedimentary delivery from the local rivers of the Raukumara Peninsula [Joanne, 2008].

9. Conclusion

[71] The Matakaoa Submarine Instability Complex (MSIC) is a system of four MTDs (Mass Transport Deposits) with a total bulk volume of 3200 km³. The MTDs were emplaced during three failure events: (1) the Raukumara Slump; (2) the Matakaoa Debris Avalanche (MDA); and (3) the Matakaoa Debris Flow (MDF), all occurring along the Matakaoa Margin, approximately 50–70 km west of the northern Hikurangi-southern Kermadec subduction margin, NE New Zealand. The successive failures resulted in the formation of the 45-km-wide, 1100-m-high Matakaoa Reentrant which conspicuously cuts the continental slope north of the Raukumara Peninsula. A volume budget shows the importance of using compacted volumes of solid rather than bulk volumes when comparing events of various origins, ages and natures globally. Compacted volumes indicate that the three components of the MSIC contributed to the formation of the reentrant, and that the reentrant was not completely healed before the subsequent mass failure.

[72] The occurrence of the Raukumara Slump is roughly dated during the Pliocene. The slump formed as the result of the collapse of the northern part of the margin. The distal part of the slump extends at least 50 km into the Raukumara Basin and forms a series of imbricate structures that deformed basin sediments into a locally confined landslide. As most of the proximal structures of the Raukumara Slump was eroded by subsequent events, the 1150 km³ compacted volume is underestimated.

[73] The Matakaoa Debris Avalanche (MDA) was emplaced 600 ± 150 ka ago. It consists of blocky and weakly reflective seismic units with a compacted volume of 280 km³ that infill the eastern half of the reentrant. The avalanche overlies a flat décollement characterized by a distinctive high-amplitude, negative-polarity seismic reflector which truncates the underlying sedimentary units, whereas rotational geometries and overlying back-tilted blocks indicate a mechanism of slump failure. During emplacement, the indurated Mio-Pliocene sedimentary basement blocks, piled up against the Tokata Anticline outcropping in the sliding path,

and resulted in the blocks thrusting onto each other. The MDA partly ran over or around the anticline and extended northward into the Raukumara Basin. Weakly developed deformation in front of the debris avalanche suggests that deformation propagated over the décollement for ~20 km into the sediments of the Raukumara Basin, but resulted in a very small amount of translational movement.

[74] The Matakaoa Debris Flow (MDF) occurred between 38 and 100 ka. It extends 200 km from the head scarp of the Matakaoa Margin and is characterized by a chaotic, low-amplitude seismic facies, covering an area of 9600 km^2 essentially in the Raukumara Basin. The 500 km^3 compacted volume of the MDF includes up to 30% of the transported material that was accreted during emplacement through basal and lateral erosion. The emplacement of the MDF was associated with intense basal erosion in its proximal part.

[75] The emplacement of the MSIC was controlled by compressional tectonic and sedimentary processes associated with (1) shortening and intense seismic activity along the Pacific-Australia plate boundary, (2) uplift of the Raukumara Peninsula, (3) subsidence in the Raukumara Basin, and (4) very high sedimentation rates on the shelf and slope. These factors enabled the generation of successive large, potentially catastrophic submarine landslides over the last 5 Ma. Such mass-failure events were associated with high-energy emplacement in a fore-arc basin, and occurred in a tectonically active environment.

Acknowledgments

References

Addington, L. D., S. A. Kuehl, and J. E. McNinch (2007), Contrasting modes of shelf sediment dispersal off a high-yield river: Waiapu River, New Zealand, *Mar. Geol.*, *243*(1–4), 18–30, doi:10.1016/j.margeo.2007.04.018.

Canals, M., et al. (2004), Slope failure dynamics and impacts from seafloor and shallow sub-seafloor geophysical data: Case studies from the COSTA project, *Mar. Geol.*, *213*, 9–72, doi:10.1016/j.margeo.2004.10.001.

Carter, L. (2001), A large submarine debris flow in the path of the Pacific deep western boundary current off New Zealand, *Geo Mar. Lett.*, *21*, 42–50.

Carter, L., and I. N. McCave (2002), Eastern New Zealand drifts: Miocene to recent, in *Deep-Water Contourites: Modern Drifts and Ancient Series, Seismic and Sedimentary Characteristics*, Geol. Soc. Mem., vol. 22, edited by D. A. V. Stow et al., pp. 101–103, Geol. Soc., London.

Chiswell, S. M., and D. Roemmich (1998), The East Cape current and two eddies: A mechanism for larval retention?, *N. Z. J. Mar. Freshwater Res.*, *32*(3), 385–397.

Cochran, U. A., et al. (2006), Paleoecological insights into subduction zone earthquake occurrence, eastern North Island, New Zealand, *Geol. Soc. Am. Bull.*, *118*(9/10), 1051–1074, doi:10.1130/B55761.1.

Coleman, J. M., and D. B. Prior (1988), Mass wasting on continental margins, *Annu. Rev. Earth Planet. Sci.*, *16*, 101–119.

Collot, J.-Y., and B. W. Davy (1998), Forearc structures and tectonics regimes at the oblique subduction zone between the Hikurangi Plateau and the southern Kermadec margin, *J. Geophys. Res.*, *103*(B1), 623–650.

Collot, J.-Y., et al. (1996), From oblique subduction to intra-continental transpression: Structures of the southern Kermadec-Hikurangi margin from multibeam bathymetry, side scan sonar and seismic reflection, *Mar. Geophys. Res.*, *18*, 357–381.

Collot, J.-Y., K. B. Lewis, G. Lamarche, and S. Lallemand (2001), The giant Ruatoria debris avalanche on the Northern Hikurangi Margin, New Zealand: Result of oblique seamount subduction, *J. Geophys. Res.*, *106*(B9), 19,271–19,297.

Dade, W. B., and H. E. Huppert (1998), Long-runout rockfalls, *Geology*, *26*(9), 803–806.

Dasgupta, P. (2003), Sediment gravity flow—The conceptual problem, *Earth Sci. Rev.*, *62*, 265–281.

Davey, F. J., S. Henrys, and E. Lodolo (1997), A seismic crustal section across the East Cape convergent margin, New Zealand, *Tectonophysics*, *269*(3–4), 199–215.

Davy, B. W. (1992), The influence of subducting plate buoyancy on subduction of the Hikurangi-Chatham Plateau beneath North Island, New Zealand, in *Geology and Geophysics of Continental Margins*, edited by J. S. Watkins, F. Zhiqiang, and K. J. McMillen, AAPG Mem., 53, 75–91.

De Blasio, F. V., A. Elverhøi, L. E. Engvik, D. Issler, P. Gauer, and C. Harbitz (2006), Understanding the high mobility of subaqueous debris flows, *Nor. Geol. Tidsskr.*, *86*(3), 275–284.

De Mets, C., R. G. Gordon, D. F. Argus, and S. Stein (1994), Effect of recent revisions to the geomagnetic reversal time scale on estimates of current plate motions, *Geophys. Res. Lett.*, *21*(20), 2191–2194.

Felix, M., and J. Peakall (2006), Transformation of debris flows into turbidity currents: Mechanisms inferred from laboratory experiments, *Sedimentology*, *53*(1), 107–123.

Field, B. D., et al. (1997), *Cretaceous-Cenozoic geology and petroleum systems of the East Coast region, New Zealand*, 301 pp., Inst. of Geol. and Nucl. Sci., Lower Hutt, New Zealand.

Frey-Martinez, J., J. A. Cartwright, and D. James (2006), Frontally confined versus frontally emergent submarine landslides: A 3D seismic characterisation, *Mar. Pet. Geol.*, *23*, 585–604, doi:10.1016/j.marpetgeo.2006.04.002.

Gibb, J. G. (1981), Coastal hazard mapping as a planning technique for Waiapu County, East Coast, North Island, New Zealand, *Water Soil Tech. Publ.*, *21*, p. 63, Natl. Water and Soil Conserv. Organ., Wellington, New Zealand.

Gillies, P. N., and F. J. Davey (1986), Seismic reflection and refraction studies of the Raukumara forearc basin, New Zealand, *N. Z. J. Geol. Geophys.*, *29*, 391–403.

Haflidason, H., R. Lien, H. P. Sejrup, C. F. Forsberg, and P. Bryn (2005), The dating and morphometry of the Storegga Slide, *Mar. Pet. Geol.*, *22*, 123–136, doi:10.1016/j.marpetgeo.2004.10.008.

Hampton, M. A., H. J. Lee, and J. Locat (1996), Submarine landslides, *Rev. Geophys.*, *34*(1), 33–60.

Hicks, D. M., and U. Shankar (2003), Sediment yield from New Zealand rivers, NIWA chart, *Misc. Ser. 79*, Natl. Water and Soil Conserv. Organ., Wellington, New Zealand.

Ilstad, T., A. Elverhøi, D. Issler, and J. G. Marr (2004), Subaqueous debris flow behavior and its dependence on the sand/clay ratio: A laboratory study using particle tracking, *Mar. Geol.*, *213*(1–4), 415–438.

Jenner, K. A., D. J. W. Piper, D. C. Campbell, and D. C. Mosher (2007), Lithofacies and origin of late Quaternary mass transport deposits in submarine canyons, central Scotian Slope, Canada, *Sedimentology*, *54*(1), 19–38, doi:10.1111/j.1365-3091.2006.00819.x.

Joanne, C. (2008), Le complexe d'instabilitiés sous-marines de Matakaoa, au large d'East Cape, Nouvelle-Zélande. Processus de transport en masse et impact des méga-instabilités sur l'architecture de l'évolution de la marge continentale, Ph.D. thesis, Univ. of Nice-Sophia Antipolis, Nice, France.

Kohn, B. P., and G. P. Glasby (1978), Tephra distribution and sedimentation rates in the Bay of Plenty, New Zealand, *N. Z. J. Geol. Geophys.*, *21*, 49–70.

Lewis, K. B., and B. A. Marshall (1996), Seep faunas and other indicators of methane-rich dewatering on New Zealand convergent margins, *N. Z. J. Geol. Geophys.*, *39*, 181–200.

Lewis, K. B., S. Lallemand, and L. Carter (2004), Collapse in a Quaternary shelf basin off East Cape, New Zealand: Evidence for passage of a subducted seamount inboard of the Ruatoria giant avalanche, *N. Z. J. Geol. Geophys.*, *47*(3), 415–429.

Lowe, D. J., P. R. Shane, B. V. Alloway, and R. M. Newnham (2008), Fingerprints and age models for widespread New Zealand tephra marker beds erupted since 30,000 years ago: A framework for NZ-INTIMATE, *Quat. Sci. Rev.*, *27*, 95–126, doi:10.1016/j.quascirev.2007.01.013.

Marr, J. G., G. Shanmugam, and G. Parker (2001), Experiments on subaqueous sandy gravity flows: The role of clay and water content in flow dynamics and depositional structures, *Geol. Soc. Am. Bull.*, *113*(11), 1377–1386.

Maslin, M., N. Mikkelsen, C. Vilela, and B. Haq (1998), Sea-level- and gas-hydrate-controlled catastrophic sediment failures of the Amazon Fan, *Geology*, *26*(12), 1107–1110.

Masson, D. G., M. Canals, B. Alonso, R. Urgeles, and V. Huhnerbach (1998), The Canary Debris Flow: Source

area morphology and failure mechanisms, *Sedimentology*, *45*(2), 411–432.

Masson, D. G., A. B. Watts, M. J. R. Gee, R. Urgeles, N. C. Mitchell, T. P. Le Bas, and M. Canals (2002), Slope failures on the flanks of the western Canary Islands, *Earth Sci. Rev.*, *57*, 1–35.

Mazengarb, C., and I. G. Speden (2000), Geology of the Raukumara Area, *Geol. Map 6*, scale 1:250,000, 1 sheet + 60 pp., Inst. of Geol. and Nucl. Sci. Ltd., Lower Hutt, New Zealand.

McAdoo, B. G., L. F. Pratson, and D. L. Orange (2000), Submarine landslide geomorphology, US continental slope, *Mar. Geol.*, *169*, 103–136.

McHugh, C. M. G., J. E. Damuth, and G. S. Mountain (2002), Cenozoic mass-transport facies and their correlation with relative sea-level change, New Jersey continental margin, *Mar. Geol.*, *184*(3–4), 295–334.

Mohrig, D., and J. G. Marr (2003), Constraining the efficiency of turbidity current generation from submarine debris flows and slides using laboratory experiments, *Mar. Pet. Geol.*, *20*(6–8), 883–899, doi:10.1016/j.marpetgeo.2003.03.002.

Mohrig, D., A. Elverhøi, and G. Parker (1999), Experiments on the relative mobility of muddy subaqueous and subaerial debris flows, and their capacity to remobilize antecedent deposits, *Mar. Geol.*, *154*(1–4), 117–129.

Moore, J. G., D. A. Clague, R. T. Holcomb, P. W. Lipman, W. R. Normark, and M. E. Torresan (1989), Prodigious submarine landslides on the Hawaiian Ridge, *J. Geophys. Res.*, *94*(B12), 17,465–17,484.

Moore, J. G., W. R. Normark, and R. T. Holcomb (1994), Giant Hawaiian underwater landslides, *Science*, *264*, 46–47.

Moscardelli, L., L. Wood, and P. Mann (2006), Mass-transport complexes and associated processes in the offshore area of Trinidad and Venezuela, *AAPG Bull.*, *90*(7), 1059–1088, doi:10.1306/02210605052.

Mulder, T., and P. Cochonat (1996), Classification of offshore mass movements, *J. Sediment. Res., Sect. A*, *66*(1), 43–57.

Nardin, T. R., F. J. Hein, D. S. Gorsline, and B. D. Edwards (1979), A review of mass movements processes, sediment and acoustic characteristics, and contrasts in slope and base-of-slope systems versus canyon-fan-basin floor system, in *Geology of Continental Slopes*, edited by L. J. Doyle and O. H. Pilkey Jr., *Spec. Publ. Soc. Econ. Paleontol. Mineral.*, *27*, 67–73.

Orpin, A. R. (2004), Holocene sediment deposition on the Poverty-slope margin by the muddy Waipaoa River, East Coast New Zealand, *Mar. Geol.*, *209*, 69–90, doi:10.1016/j.margeo.2004.06.001.

Orpin, A. R., C. Alexander, L. Carter, S. Kuehl, and J. P. Walsh (2006), Temporal and spatial complexity in post-glacial sedimentation on the tectonically active, Poverty Bay continental margin of New Zealand, *Cont. Shelf Res.*, *26*, 2205–2224, doi:10.1016/j.csr.2006.07.029.

Piper, D. J. W., and C. McCall (2003), A synthesis of the distribution of submarine mass movements on the eastern Canadian margin, in *Submarine Mass Movements and Their Consequences*, 1st *International Symposium*, edited by J. Locat and J. Mienert, pp. 291–298, Kluwer Acad., New York.

Piper, D. J. W., C. Pirmez, P. L. Manley, D. Long, R. D. Flood, W. R. Normark, and W. Showers (1997), Mass transport deposits of the Amazon fan, *Proc. Ocean Drill. Program Sci. Results*, *155*, 109–146.

Piper, D. J. W., P. Cochonat, and M. L. Morrison (1999), The sequence of events around the epicentre of the 1929 Grand Banks earthquake: Initiation of debris flows and turbidity

current inferred from sidescan sonar, *Sedimentology*, *46*(1), 79–97.

Prior, D. B., B. D. Bornhold, and M. W. Johns (1984), Depositional characteristics of submarine debris flow, *J. Geol.*, *92*, 707–727.

Proust, J.-N., G. Lamarche, S. Migeon, and H. Neil (2006), Campagne GEOSCIENCES: MD152 (24 January– 7 February 2006) on R/V Marion-Dufresne, "Tectonic and climatic controls on sediment budget," Cruise Report, 108 pp., Inst. Paul Emile Victor, Brest, France.

Reyners, M. (1998), Plate coupling and the hazard of large subduction thrust earthquakes at the Hikurangi subduction zone, New Zealand, *N. Z. J. Geol. Geophys.*, *41*, 343–354.

Reyners, M., and P. McGinty (1999), Shallow subduction tectonics in the Raukumara Peninsula, New Zealand, as illuminated by earthquake focal mechanisms, *J. Geophys. Res.*, *104*(B2), 3025–3034.

Schwartz, H.-U. (1982), Subaqueous slope failures—Experiment and modern occurrences, in *Contributions to N. 242 of the Joint Programme 95 Interaction Sea-Sea Bottom, Kiel Univ., Germany*, edited by H. Fuchtbauer et al., pp. 1–103, Kiel Univ., Kiel, Germany.

Skempton, A. W., and J. N. Hutchinson (1969), Stability of natural slope and embankment foundations, state of the art report, in 7th *International Conference on Soil Mechanics and Foundation Engineering, Proceedings, Mexico City*, vol. 2, pp. 291–335, Soc. Mex. de Mec. de Suelos, Mexico City.

Wilson, K., K. Berryman, U. Cochran, and T. Little (2007a), Holocene coastal evolution and uplift mechanisms of the northeastern Raukumara Peninsula, North Island, New Zealand, *Quat. Sci. Rev.*, *26*(7–8), 1106–1128.

Wilson, K. J., K. R. Berryman, N. J. Litchfield, and T. A. Little (2007b), Distribution, age and uplift patterns of Pleistocene marine terraces of the northern Raukumara Peninsula, North Island, New Zealand, *N. Z. J. Geol. Geophys.*, *50*(3), 181–191.

Wood, R., and B. Davy (1994), The Hikurangi Plateau, *Mar. Geol.*, *118*, 153–173.

Wright, I. C. (1994), Nature and tectonic setting of the southern Kermadec submarine arc volcanoes: An overview, *Mar. Geol.*, *118*, 217–236.